Supplementary Information (SI) for Materials Advances.
This journal is © The Royal Society of Chemistry 2025

Cationic iridium(III) complexes with a halogen-substituted pyridylbenzimidazole ancillary ligand for photodynamic therapy

Pierre-Henri Lanoë,[a] Frédérique Loiseau,[a] Christian Philouze,[a] Camille Latouche,[b,c†] Laetitia Vanwonterghem,[d] Louis Biancon,[a] Ahmed S. Faihan,[a] Florian Molton,[a] Matéo Lavaud,[d] Anne-Laure Bulin,[d] Jean-Luc Coll,[d] Akos Banyasz,[e] Amandine Hurbin[d]**

Authors affiliation

[a] Univ. Grenoble Alpes, CNRS, DCM, 38000 Grenoble, France

[b] Nantes Université, CNRS, Institut des Matériaux de Nantes Jean Rouxel, IMN, F-44000 Nantes, France

[c] Institut Universitaire de France (IUF), F-75005 Paris, France

[d] Univ. Grenoble Alpes, INSERM U1209, CNRS UMR5309, Institute for Advanced Biosciences, 38000 Grenoble, France

[e] Laboratoire de Chimie École Normale Supérieure de Lyon, ENS, CNRS, UCBL UMR 5182, 46 Allée d'Italie, Lyon, 69364 France

* Corresponding authors: amandine.hurbin@univ-grenoble-alpes.fr and pierre-henri.lanoe@univ-grenoble-alpes.fr

[†] C. L. should be contacted for the calculation requests, Camille.Latouche@cnrs-imn.fr

Table of contents

Absorption and emission spectroscopies

Absorption spectra were recorded on a Cary 300 UV−visible spectrophotometer (Varian) and emission spectra (in solution at room temperature and in rigid matrix at 77 K) were recorded on a Horiba Fluoromax 4 or FLS-1000 Edimbrugh Instrument equipped with a photomultiplier (PMT) R928P cooled with a Peltier at -20°C. Quartz cuvettes with 1 cm optical path were used. Lifetimes were measured using LP900 spectrometer with a Flashlamp pumped by Q-switched Nd:Yag laser operating at 355 nm and with a PMT detector, or with a picosecond laser diode operating at 405 nm and using a time-correlated single photon counting detection (TCSPC, PicoHarp 300).

Emission quantum yields in solution were determined in deaerated CH_2Cl_2 or CH_3CN solutions at room temperature, and calculated with the following equation.

$$QY_s = QY_{ref} \times \frac{I_s}{I_{ref}} \times \frac{A_{ref}}{A_s} \times \left(\frac{\eta_s}{\eta_{ref}}\right)^2$$

$\mathbf{QY_s}$ corresponds to the quantum yield of the sample to be analysed, $\mathbf{QY_{ref}}$ is the quantum yield of the reference compound (in this work $[Ru(bpy)_3(PF_6)_2]$ in air equilibrated CH_3CN solution), **I** corresponds to the intensity of the emission (area of the spectrum), **A** is the absorption at the excitation wavelength, **η** corresponds to the refractive index of the solvents.

The two properties that provide information about the excited state beside the shape of the emission are the **QY** (Φ) and lifetime (τ), represented the following equations.

$$\Phi = \frac{k_r}{k_r + k_{nr}} \quad \tau = \frac{1}{k_r + k_{nr}}$$

The radiative (k_r) and non-radiative (k_r) constants can be obtained from combination and rearrangement of the **QY** (Φ) and τ equations to give equations:

$$k_r = \frac{\Phi}{\tau} \qquad k_{nr} = \frac{1}{\tau} - k_r$$

Crystal Structures Determinations and Refinements

Single crystals of compounds **Ir-H** and **Ir-Cl**, were picked up from the mother liquor, coated with a paraffin mixture, collected with nylon loops and mounted on goniometer heads. Measurements were made at 200 K on a Enraf-Nonius 4 circles kappa goniometer equipped with an Incoatec high brilliance microsource with Montel optics monochromated Mo-Kα radiation (λ = 0.71073 Å). The detector was a Bruker APEXII and an Oxford Cryosystem cryostream cooler was used. The crystal data and details of the data collections are given in Table S 1. The data were integrated and corrected for Lorentz and polarization effects using Eval141, corrected for absorption using SADABS2 and finally merged using Xprep3. Crystallographic structures were solved using direct methods implemented by Superflip.[4] Refinement was performed using ShelxL-2013[5] run under Olex2[6]. C, Cl, F, Ir, N, O, and Br atoms were refined anisotropically by the full matrix least-squares method on F2. H atoms were set geometrically.

[1] Duisenberg, A. J. M., Kroon-Batenburg, L. M. J. & Schreurs, A. M. M. (2003). *J. Appl. Cryst.* **36**, 220-229.
[2] Bruker (2004). *SADABS*. Bruker AXS Inc., Madison, Wisconsin, USA.
[3] Bruker (2005). *XPREP*. Bruker AXS Inc., Madison, Wisconsin, USA.
[4] Palatinus, L. & Chapuis, G. (2007). *J. Appl. Cryst.* **40**, 786-790.
[5] Sheldrick, G. M. (2015). *Acta Cryst.* C**71**, 3-8.
[6] Dolomanov, O.V., Bourhis, L.J., Gildea, R.J, Howard, J.A.K. & Puschmann, H. (2009), J. Appl. Cryst. 42, 339-341

Supplementary data is available on request from the CCDC, 12 Union Road, Cambridge CB2 1EZ, UK, quoting the deposition number 2338300 and 2338301 for **Ir-H and Ir-Cl** respectively. These data can be obtained free of charge at www.ccdc.cam.ac.uk/conts/retrieving.html or fax: +44-1223/336-033; E-mail: deposit@ccdc.cam.ac.uk].

Table S 1 : Crystal data and structure refinement.

Compound	**Ir-H**	**Ir-Cl**
Formula	$C_{39}H_{35}IrN_5$. (PF_6). (C_2H_3N)	$C_{39}H_{35}ClIrN_5$. (PF_6). (C_2H_3N)
F_w	951.94	986.38
T [K]	200	200
Morphology	needle	plate
Color	yellow	yellow
Crystal size [mm]	0.08 x 0.15 x 0.40	0.36 x 0.35 x 0.14
Crystal system	monoclinic	monoclinic
Space group	$P2_1/c$	$P2_1/c$
a [Å]	13.434(3)	13.384(3)
b [Å]	10.373(2)	10.828(2)
c [Å]	28.120(6)	27.667(6)
α [°]	90	90
β [°]	100.11(3)	101.07(3)
γ [°]	90	90
Unit-cell volume [Å^3]	3857.8(14)	3935.1(14)
Z	4	4
D_x [g·cm^{-3}]	1.639	1.665
μ [mm^{-1}]	3.570	3.569
Radiation [Å]	MoKα (λ = 0.71073)	MoKα (λ = 0.71073)
Θ range for data collection/°	2.524 to 27.500	2.461 to 27.500
Index ranges	$-17 \le h \le 17$, $-12 \le k \le 13$, $-34 \le l \le 36$	$-17 \le h \le 17$, $-14 \le k \le 13$, $-27 \le l \le 35$

Total reflections	48400	50690
Unique reflections	8781	8843
Used reflections (I>2σ(I))	7772	8267
Refined parameters	536	545
Rint.	0.0393	0.0318
R^a	0.0332	0.0350
$R(w)^a$	0.0657	0.0725
Goodness of fit *S*	1.142	1.339
$\Delta\rho_{min}/\Delta\rho_{max}$ (e·Å^{-3})	-1.488/2.714	-1.394/1.725

[a] Refinement based on F^2 where $w = 1/[\sigma^2(Fo^2)+(0.0129P)^2+10.0446P]$ where $P=(Fo^2+2Fc^2)/3$ for **Ir-H**

$w = 1/[\sigma^2(Fo^2)+11.8524P]$ where $P=(Fo^2+2Fc^2)/3$ for **IrCl**

NMR Spectra.

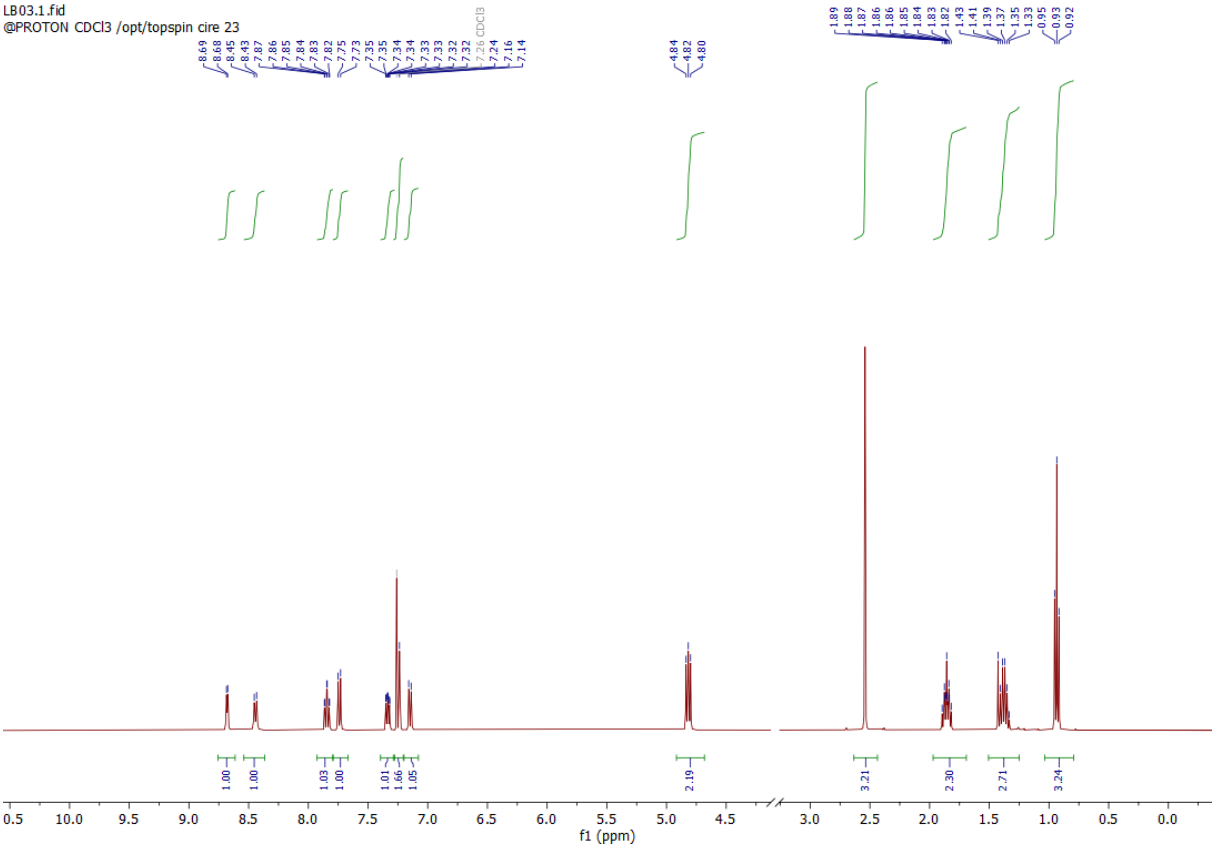

Figure S 1 : **2a** ^{1}H NMR Spectrum $CDCl_3$, 400 MHz.

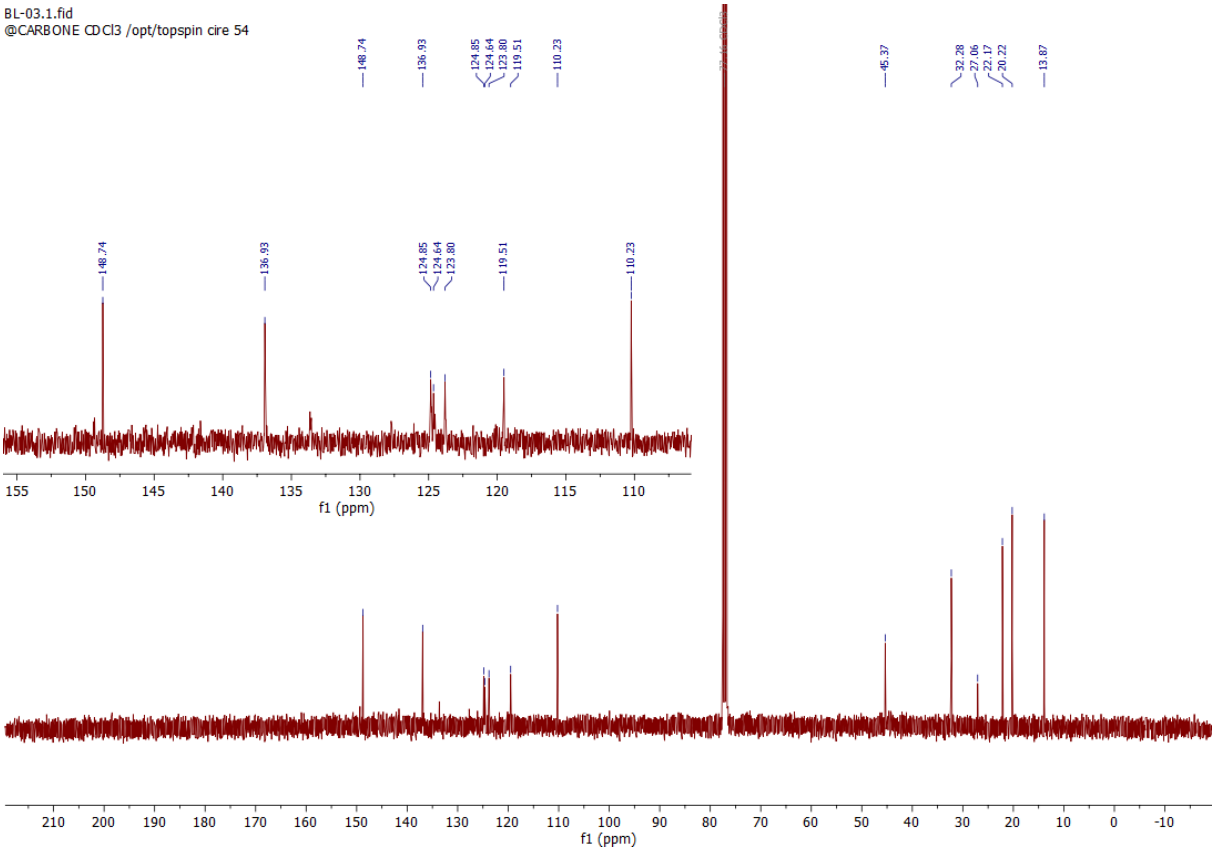

Figure S 2 : **2a** ^{13}C NMR Spectrum $CDCl_3$, 101 MHz.

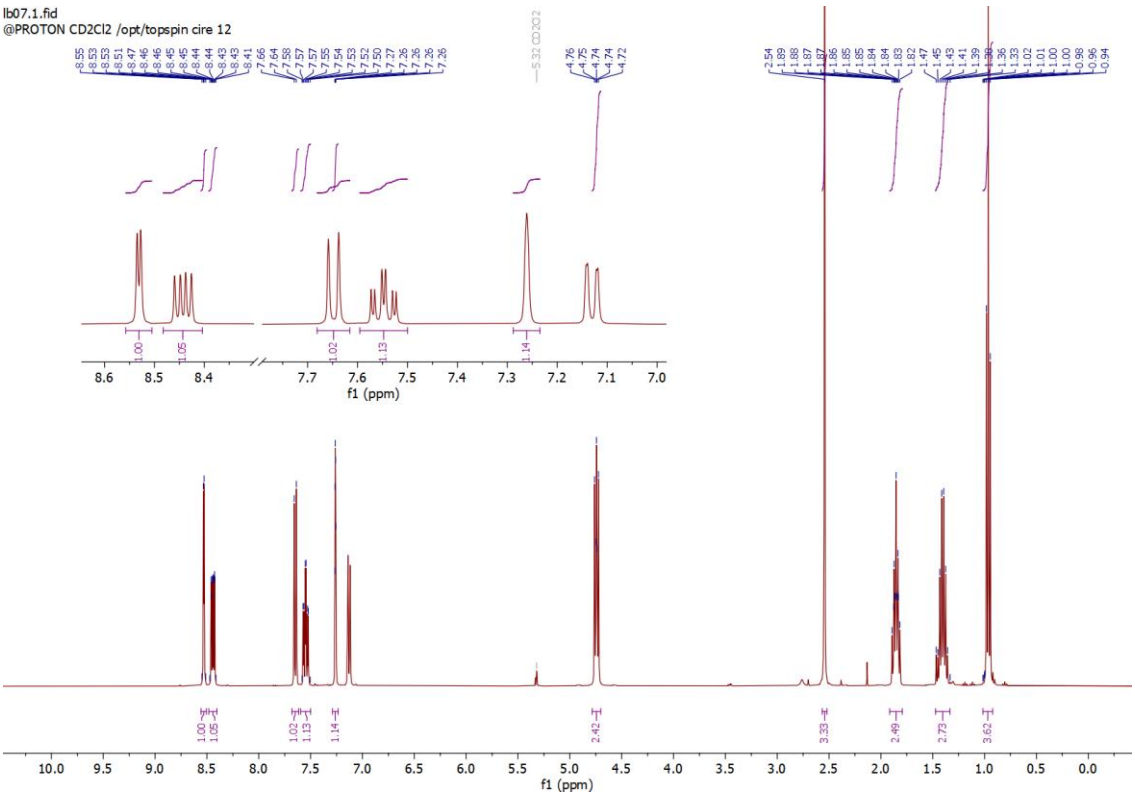

Figure S 3 : **2b** ^{1}H NMR Spectrum CD_2Cl_2, 400 MHz.

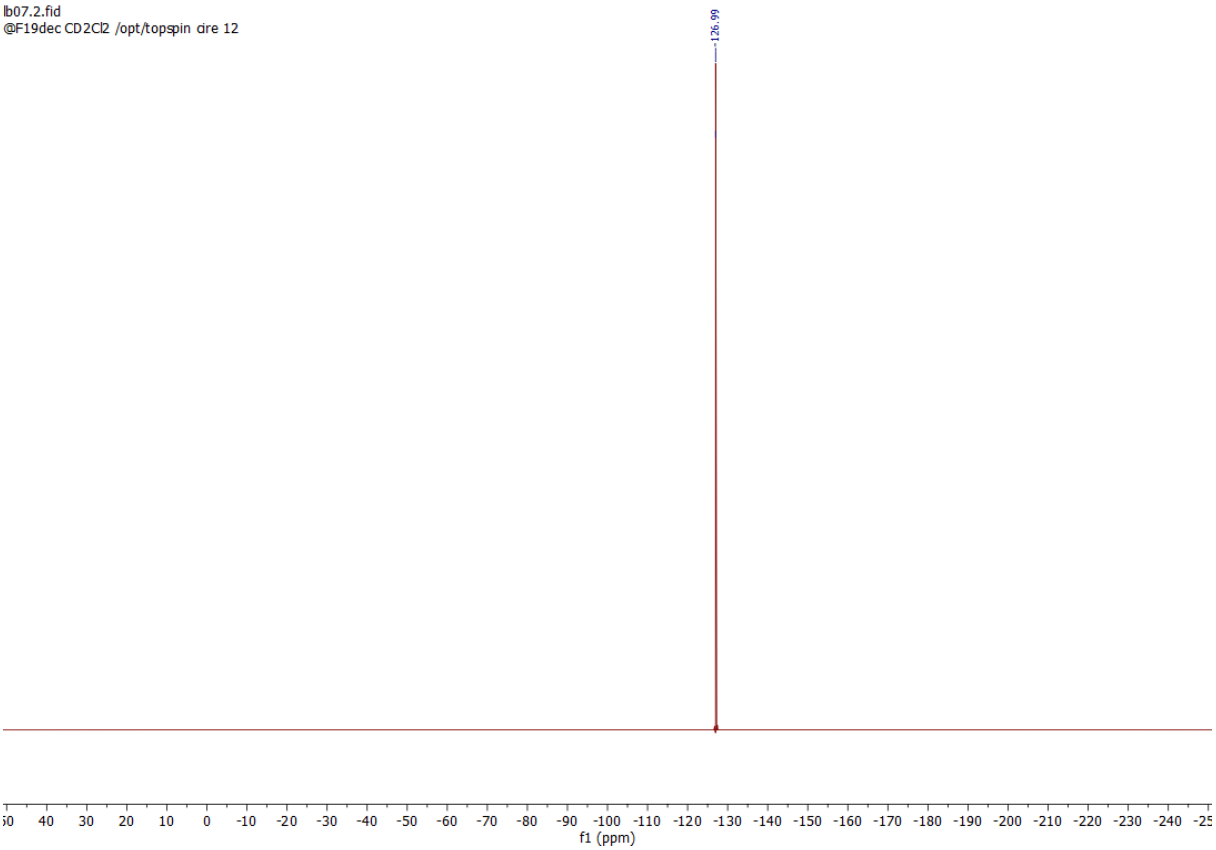

Figure S 4 : **2b** ^{19}F NMR Spectrum CD_2Cl_2, 376 MHz.

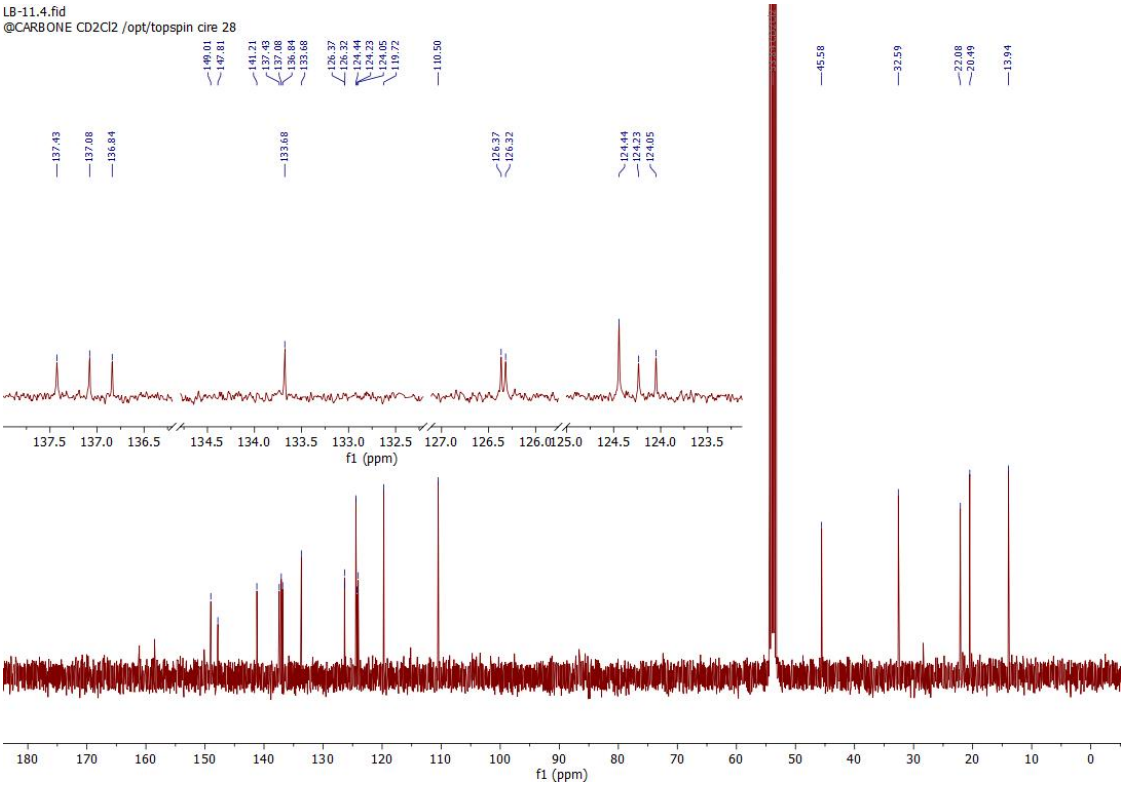

2b ^{13}C NMR Spectrum CD_2Cl_2, 101 MHz

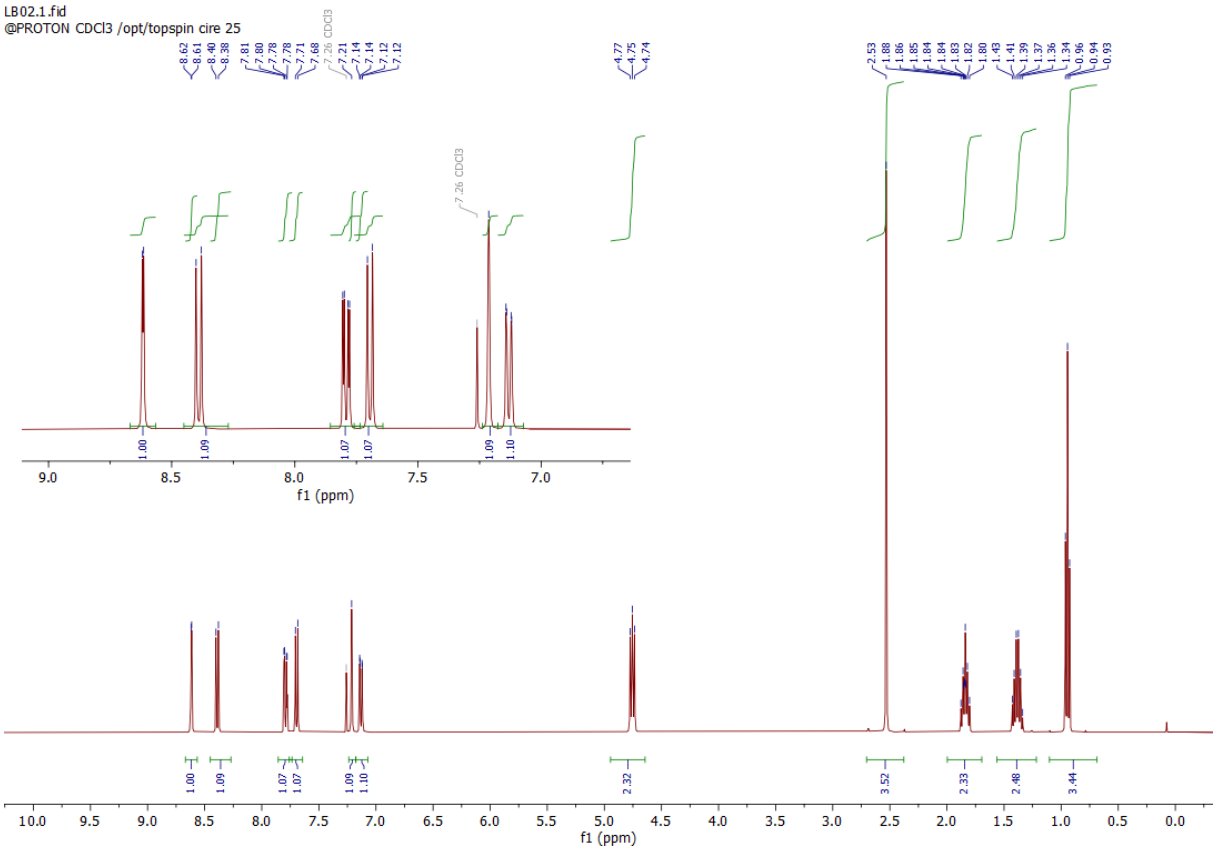

Figure S 5 : **2c** ^{1}H NMR Spectrum $CDCl_3$, 400 MHz.

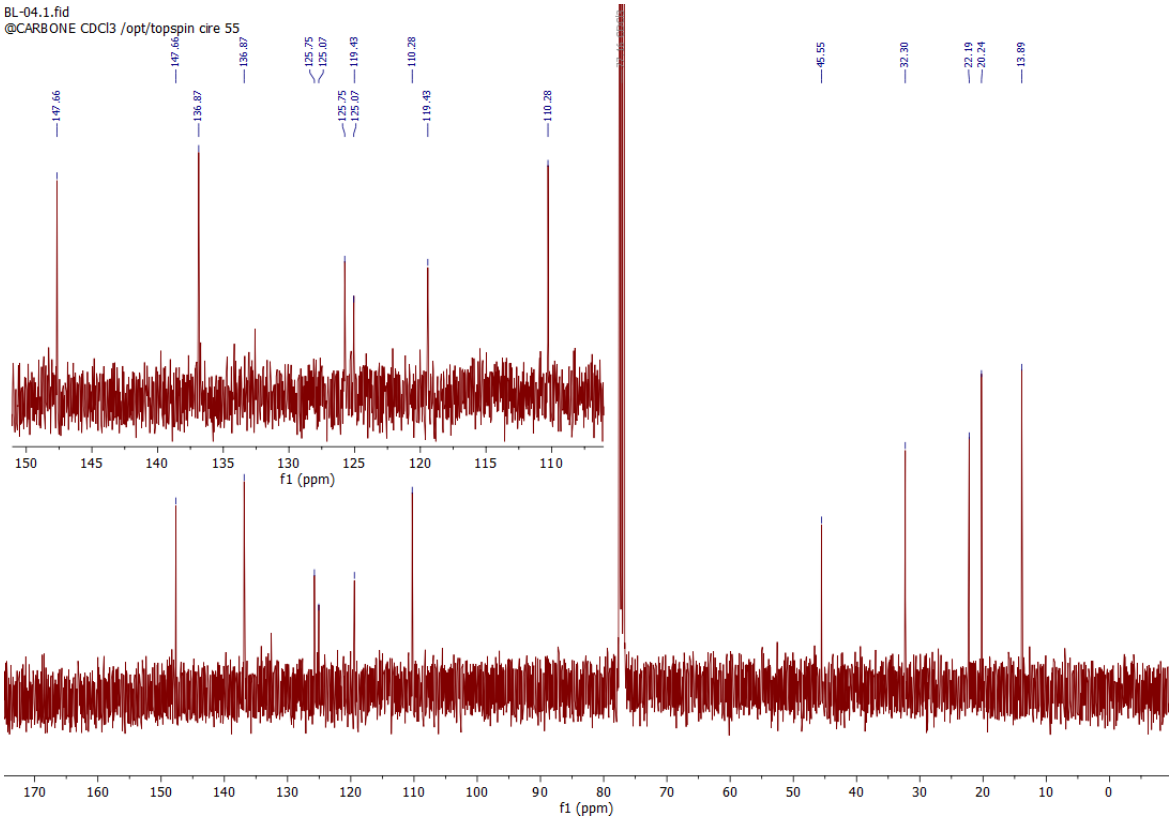

Figure S 6 : **2c** ^{13}C NMR Spectrum $CDCl_3$, 101 MHz.

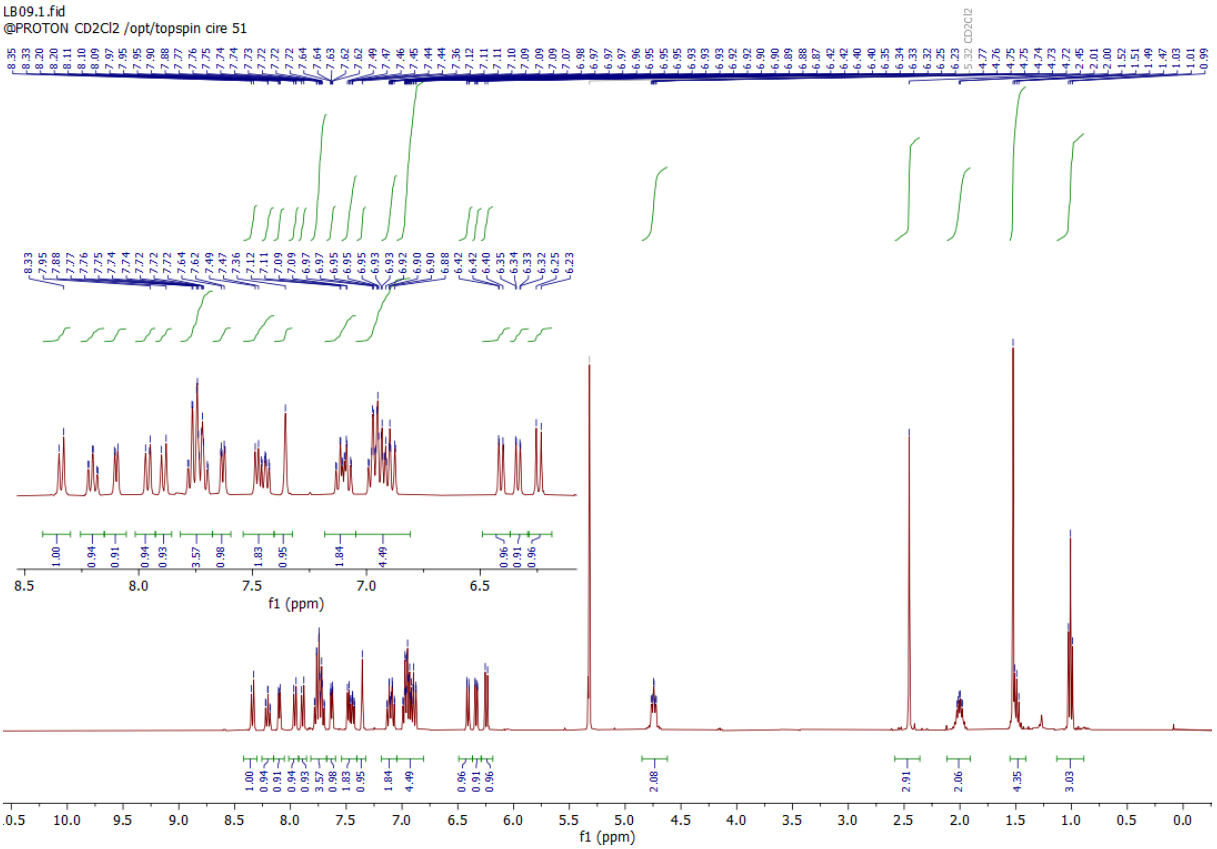

Figure S 7 : **Ir-H** ^{1}H NMR Spectrum CD_2Cl_2, 500 MHz

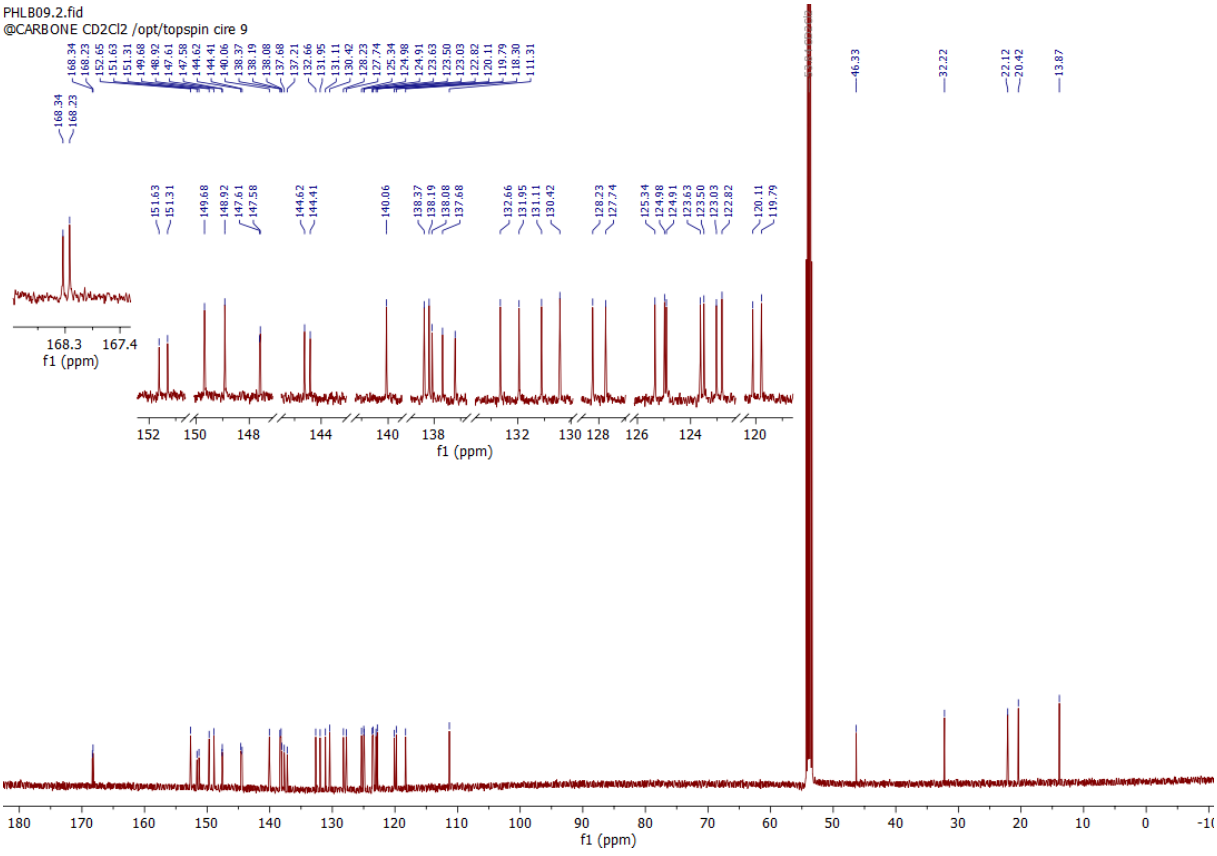

Figure S 8 : **Ir-H** ^{13}H NMR Spectrum CD_2Cl_2, 126 MHz.

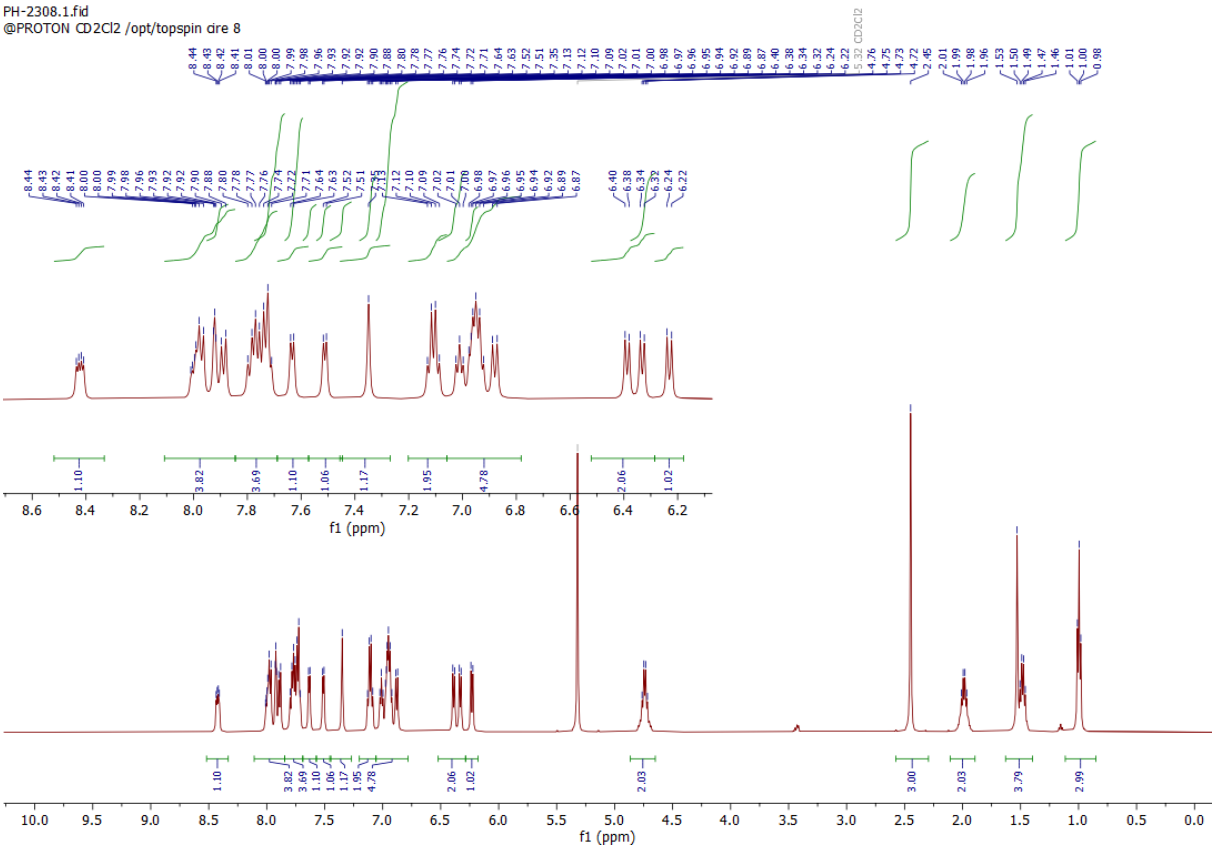

Figure S 9 : **Ir-F** ^{1}H NMR Spectrum CD_2Cl_2, 500 MHz

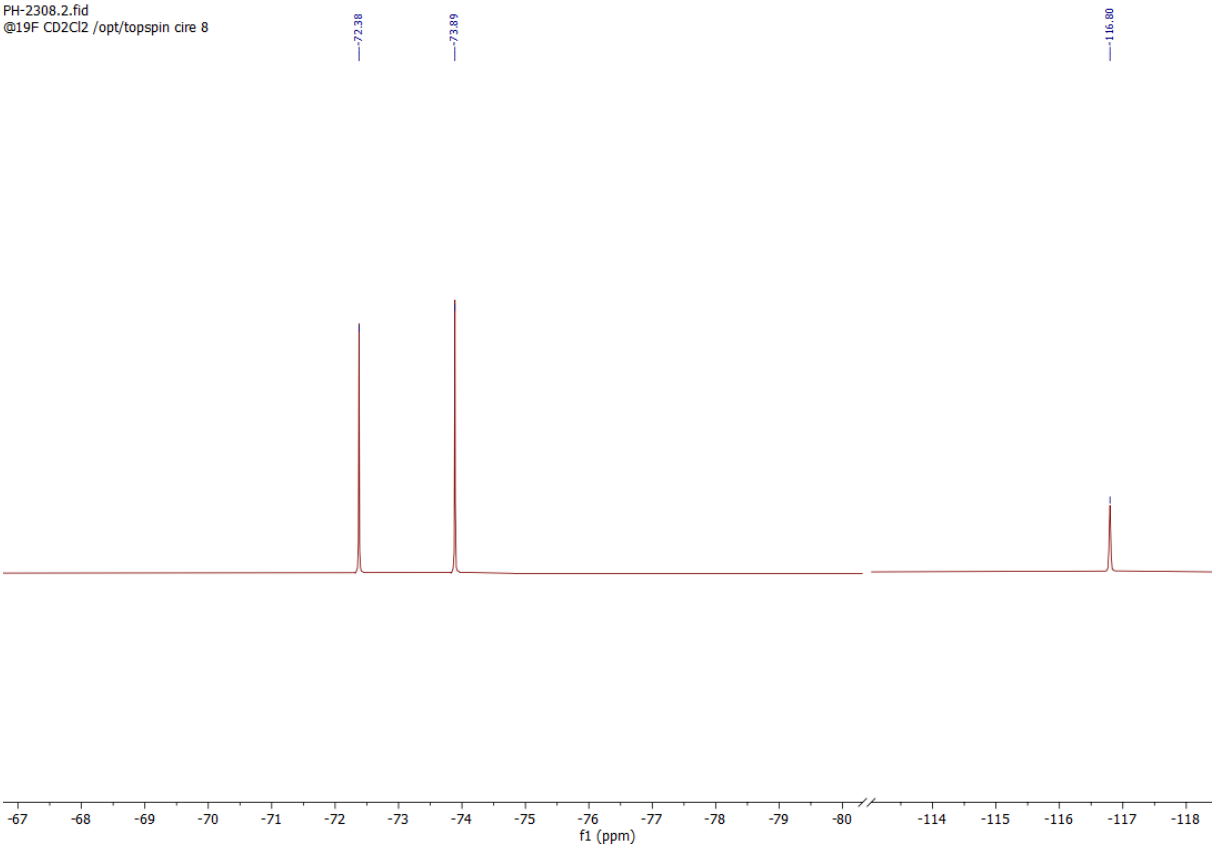

Figure S 10 : : **Ir-F** ^{19}F NMR Spectrum CD_2Cl_2, 470 MHz.

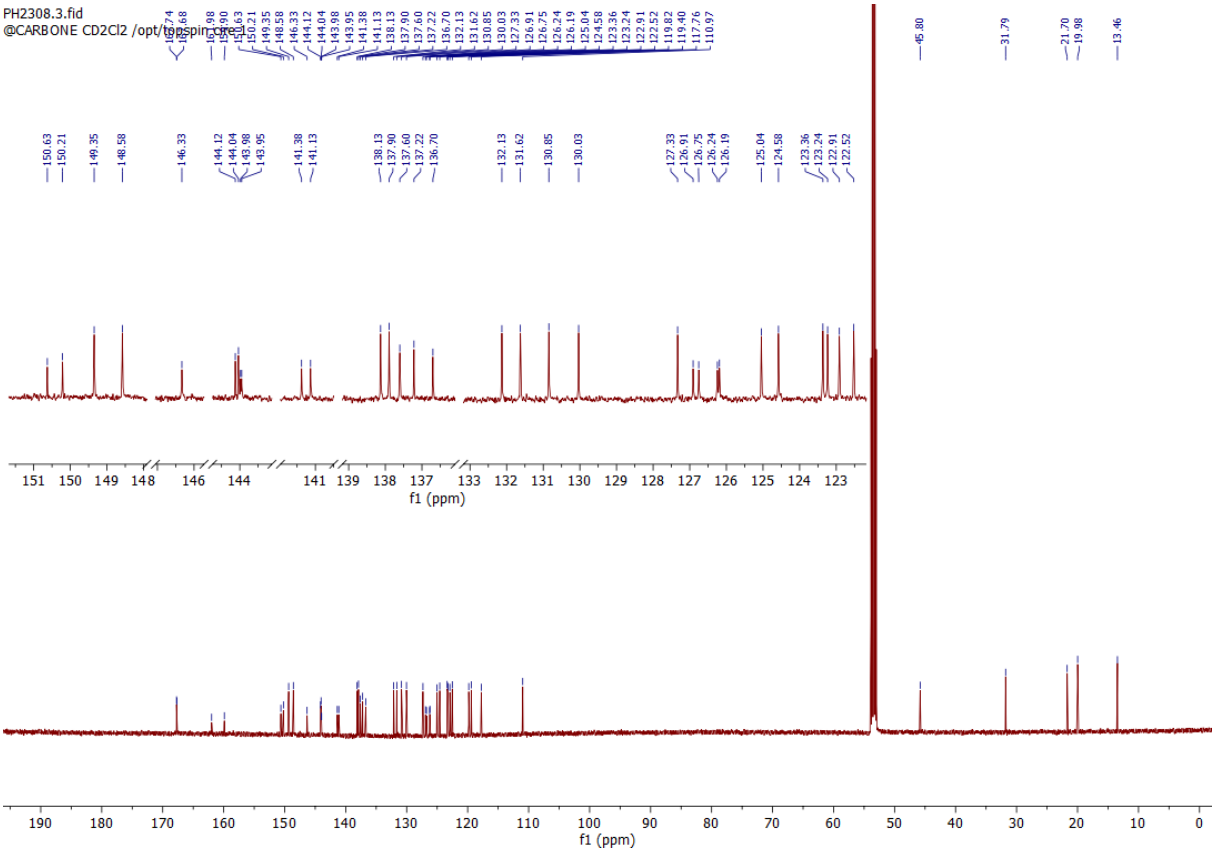

Figure S 11 : **Ir-F** ^{1}H NMR Spectrum CD_2Cl_2, 126 MHz.

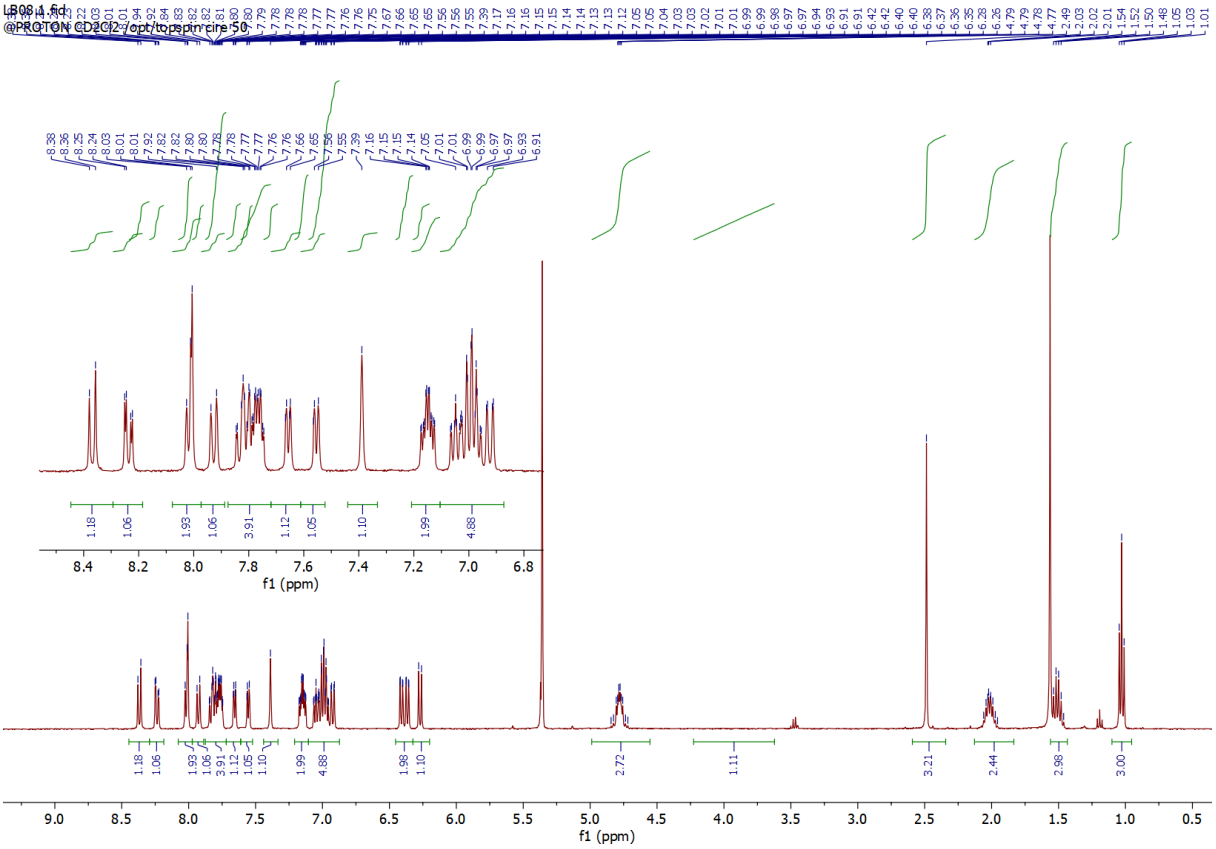

Figure S 12 : **Ir-Cl** ^{1}H NMR Spectrum CD_2Cl_2, 500 MHz.

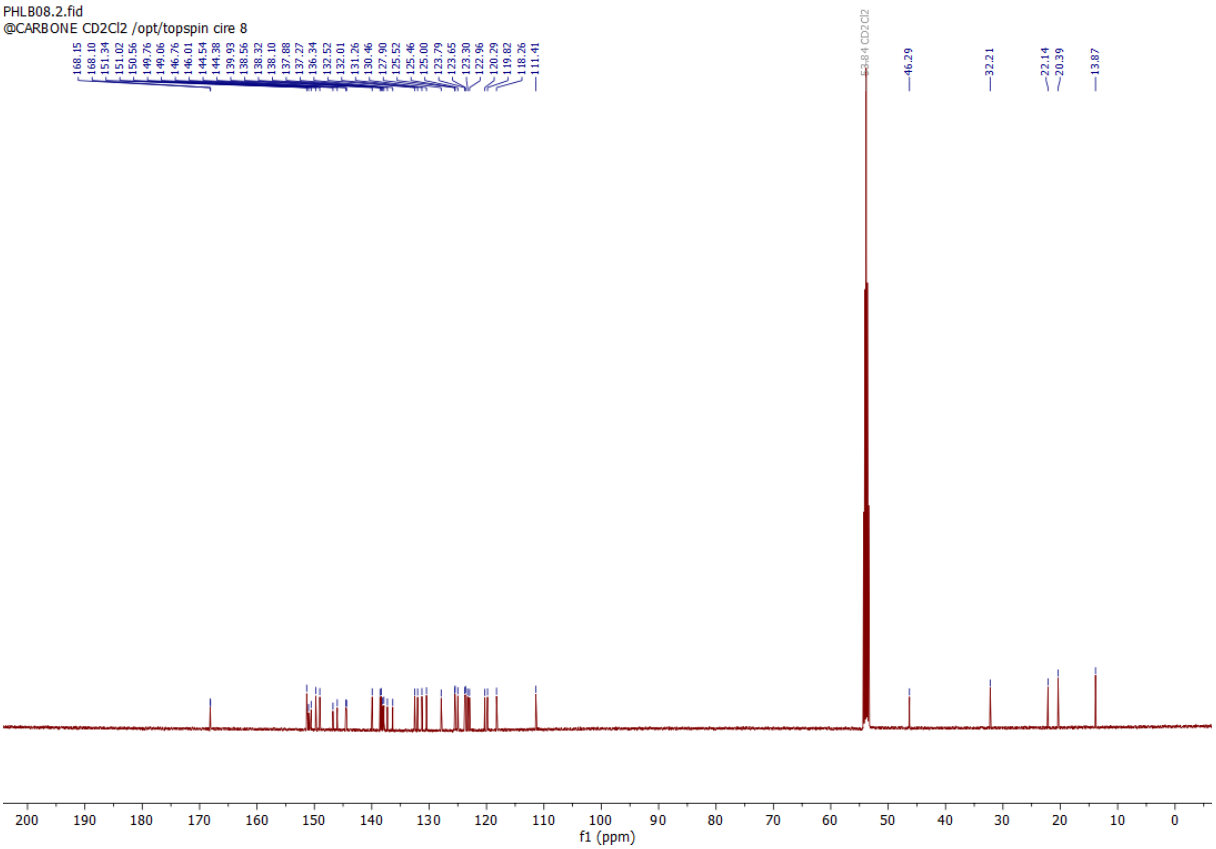

Figure S 13 : **Ir-Cl** ^{13}C NMR Spectrum CD_2Cl_2, 126 MHz.

Individual Absorption and emission (278 K and 77 K) spectra

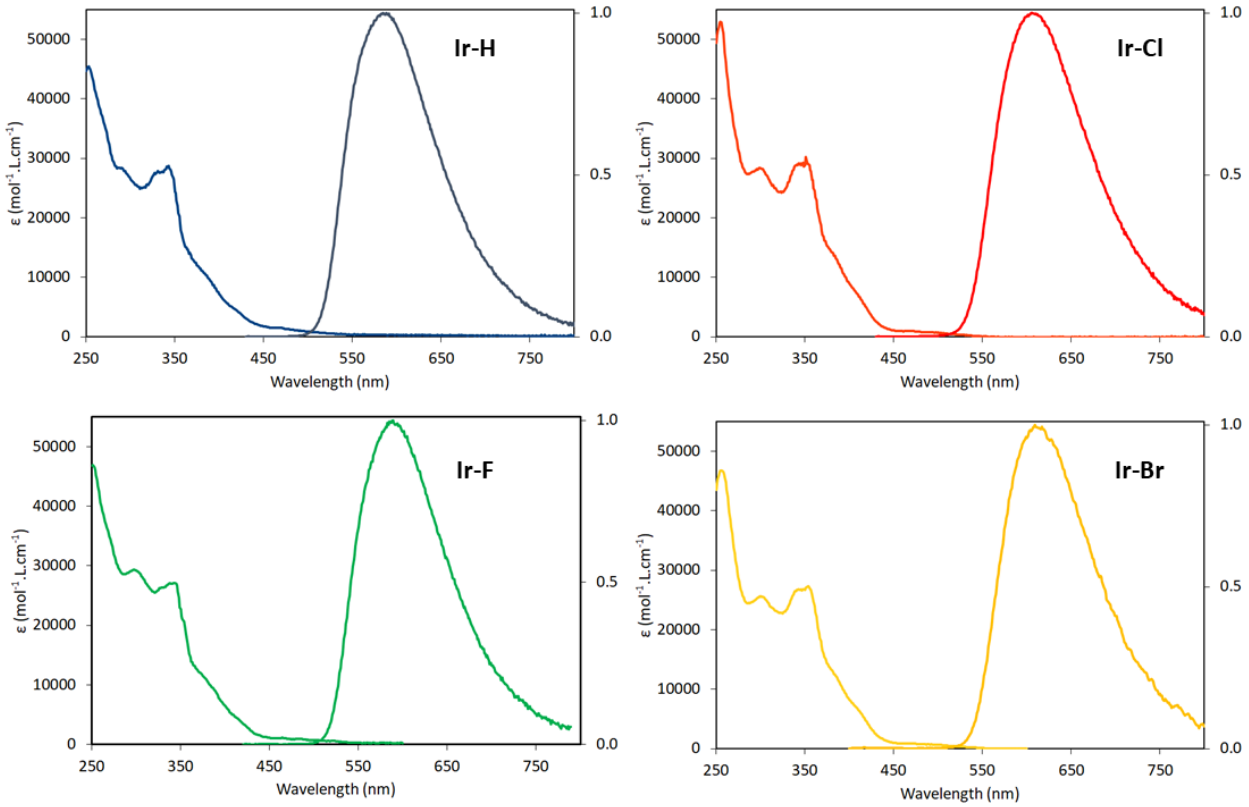

Figure S 14 : Absorption and emission spectra in CH_2Cl_2 at room temperature.

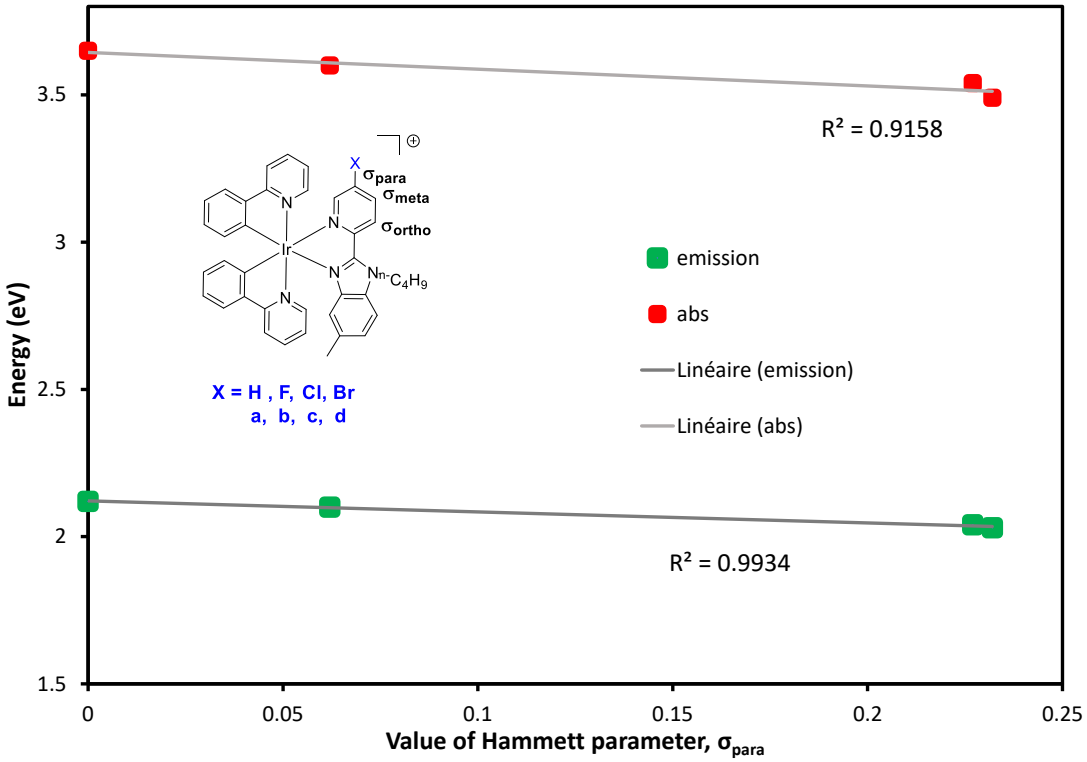

Figure S 15 : Absorption (red) and emission (green) energy in function of the Hammett parameter σ_{para}.

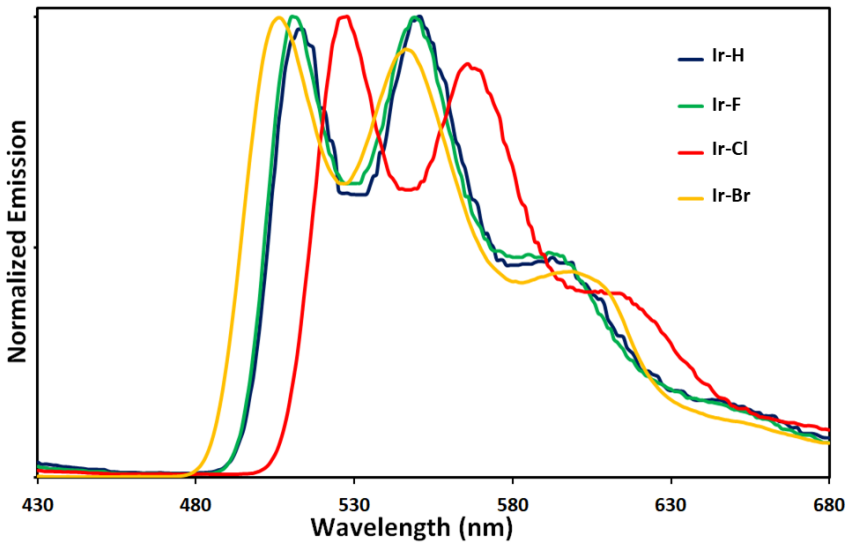

Figure S 16 : Emission spectra in butyronitrile at 77 K.

EPR spectra

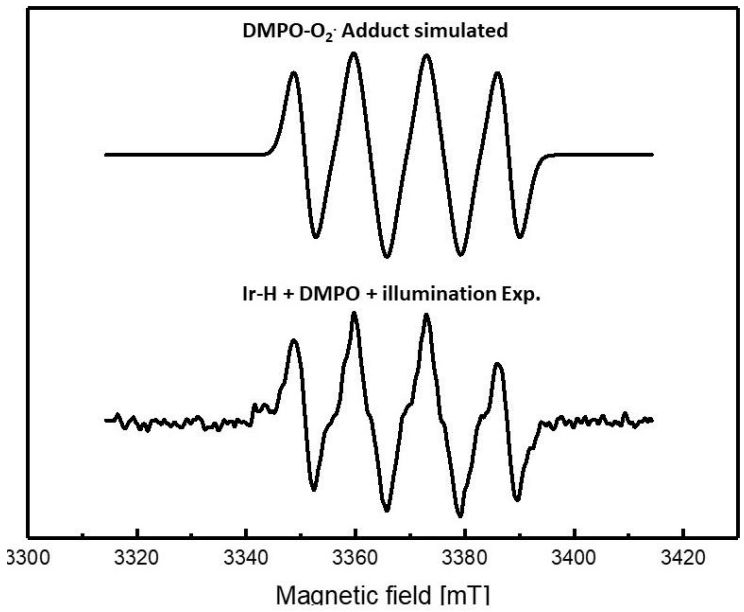

Figure S 17 : EPR spectrum of **Ir-H** + DMPO in MeOH after 5 min illumination at 420 nm with simulated spectrum of DPMO $O2^{\cdot-}$ adduct, with hyperfine coupling values: a(N) = 13.5 G, a(H) = 10.4 G.

Orbital's densities and TD-DFT band gaps

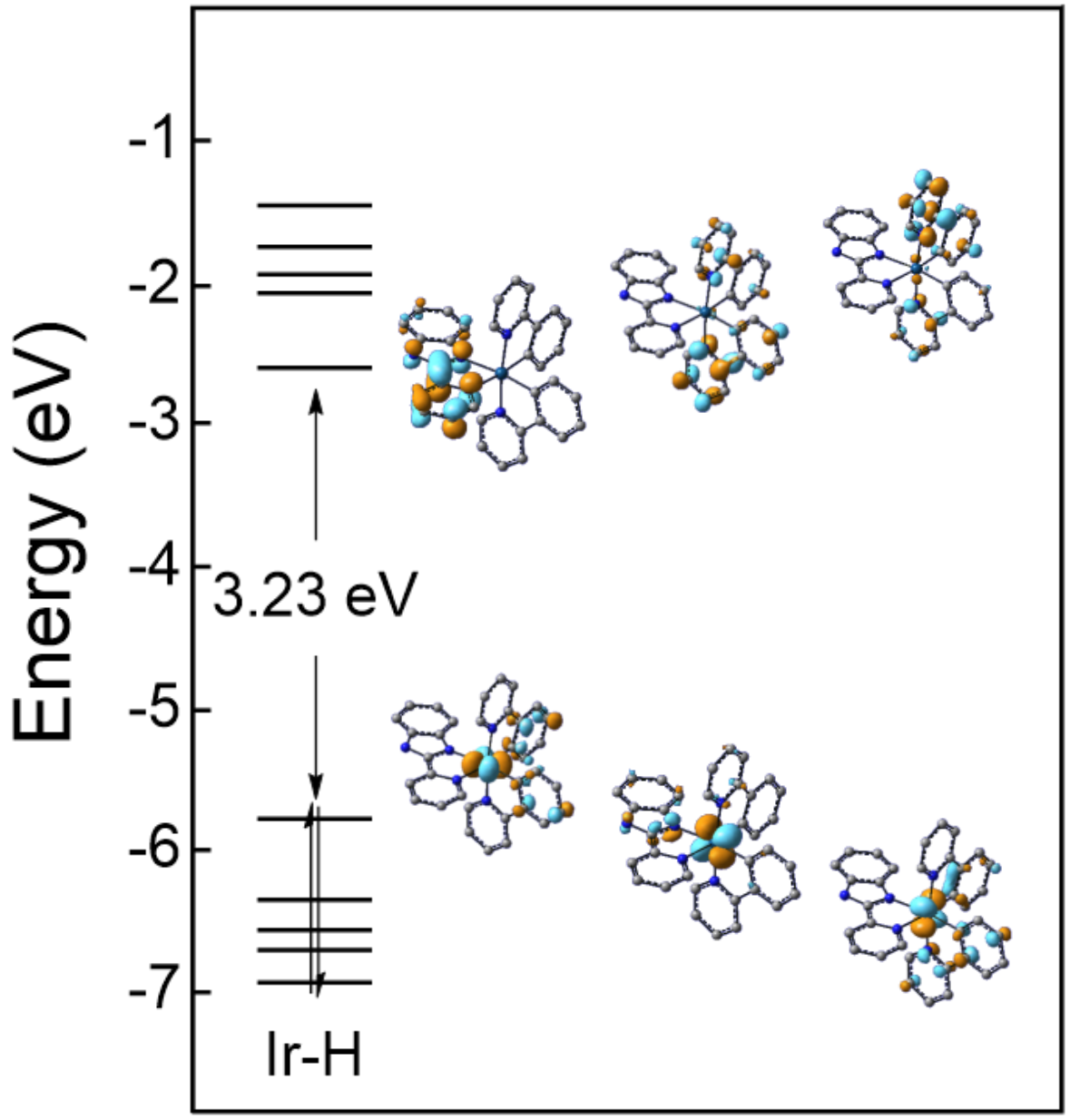

Figure S 18 : Molecular frontier orbitals of **Ir-H** together with orbital plots from HOMO-2 to LUMO+2.

Table S 2 : TD-DFT band assignment for all complexes together with oscillator strengths.

Compound	λ(nm)	f(oscillator strength)	Assignment	Transition type
Ir-H	487	0.0003	HOMO→LUMO	ML'CT +LL'CT
	406	0.0967	HOMO→LUMO+1	MLCT + LLCT
	405	0.0401	HOMO-1 → LUMO HOMO-2 → LUMO	ML'CT + L'L'CT +LL'CT
Ir-F	483	0.0005	HOMO→LUMO	ML'CT +LL'CT
	405	0.0980	HOMO→LUMO+1 HOMO → LUMO+2	MLCT + LLCT
	403	0.0393	HOMO-1 → LUMO HOMO-2 → LUMO	ML'CT + L'L'CT +LL'CT
Ir-Cl	503	0.0002	HOMO→LUMO	ML'CT +LL'CT
	416	0.0508	HOMO-1 → LUMO HOMO-2 → LUMO	MLCT + LLCT
	406	0.0946	HOMO→LUMO+1 HOMO → LUMO+2	ML'CT + L'L'CT +LL'CT
Ir-Br	505	0.0002	HOMO→LUMO	ML'CT +LL'CT
	417	0.1004	HOMO-1 → LUMO HOMO-2 → LUMO	MLCT + LLCT
	404	0.0407	HOMO→LUMO+1 HOMO → LUMO+2	ML'CT + L'L'CT +LL'CT
Ir-I	509	0.0004	HOMO→LUMO	ML'CT +LL'CT
	420	0.0644	HOMO-1 → LUMO HOMO-2 → LUMO	MLCT + LLCT
	405	0.0972	HOMO→LUMO+1 HOMO → LUMO+2	ML'CT + L'L'CT +LL'CT

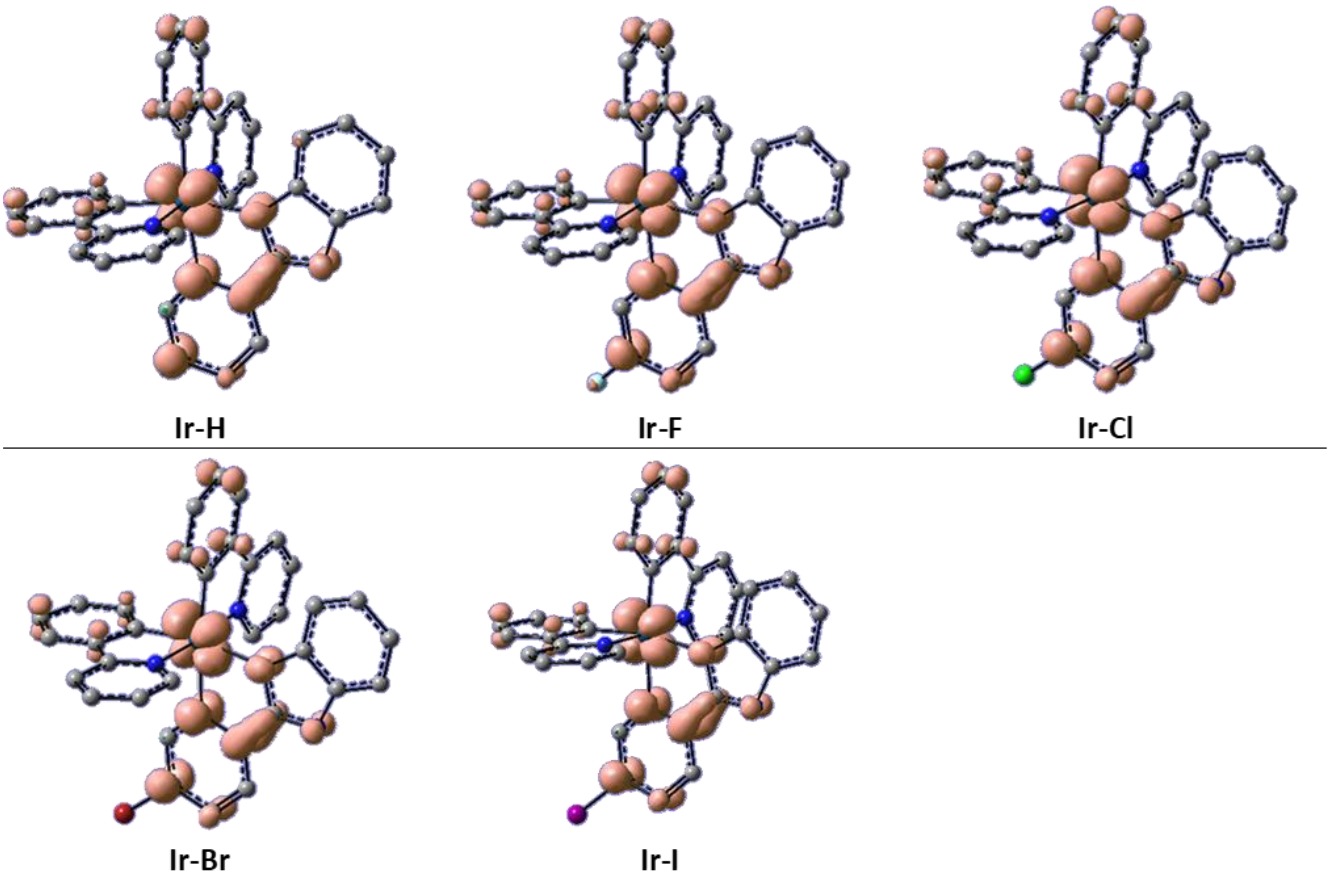

Figure S 19 : Spin densities of the investigated complexes.

Individual two-photon absorption spectra

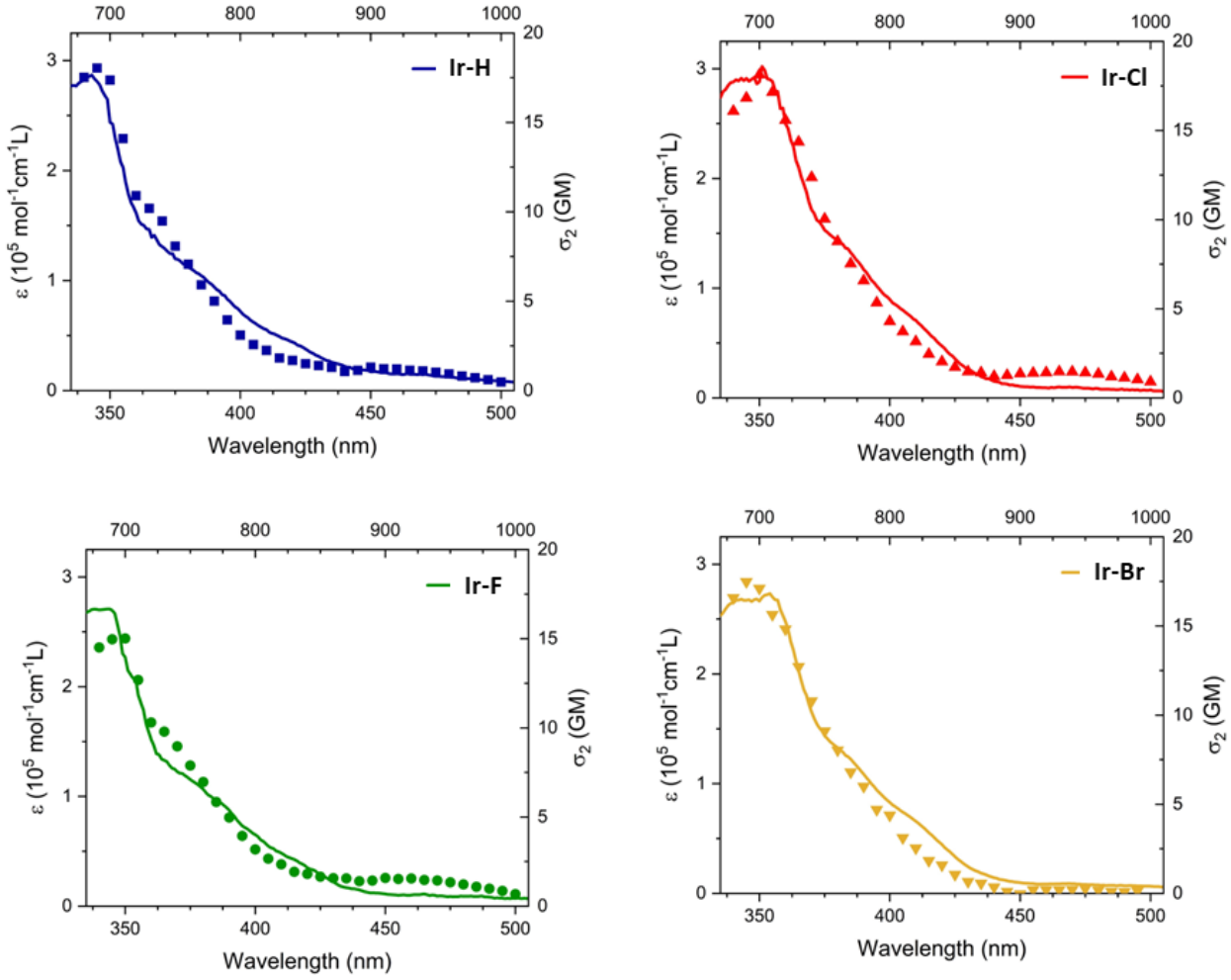

Figure S 20 : Two-photon absorption cross-section spectra of the **Ir-X** complexes measured in aerated dichloromethane solutions at room temperature.

Confocal microscopy images and phototoxicity

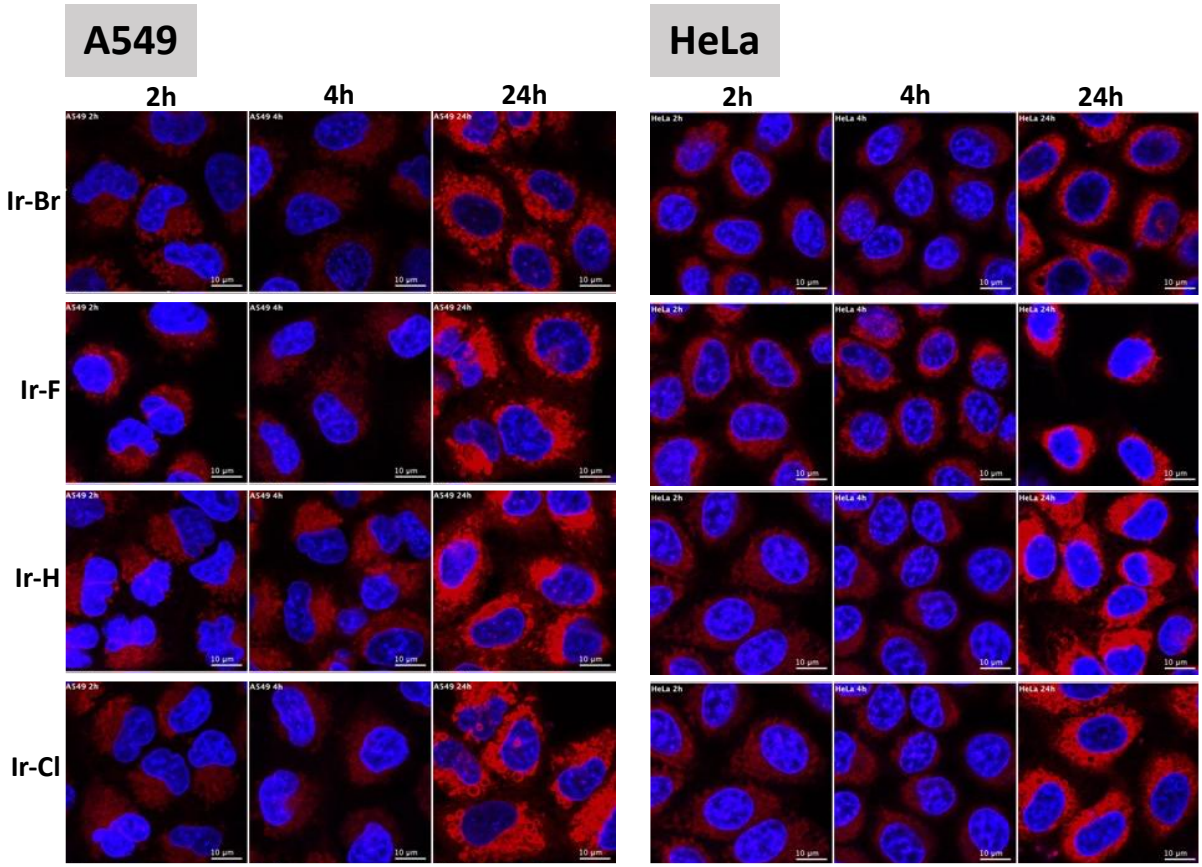

Figure S 21 : Ir(III) complexes are internalized in A549 and HeLa cells. Representative confocal microscopy images of A549 cells and HeLa incubated with 1 µmol.L^{-1} **Ir-Br**, **Ir-F, Ir-H**, and **Ir-Cl** for 2 h, 4 h or 24 h. Nuclei are stained with Hoechst 33342 (in blue). The compounds fluorescence is observed in red. Scale bars = 10 µm.

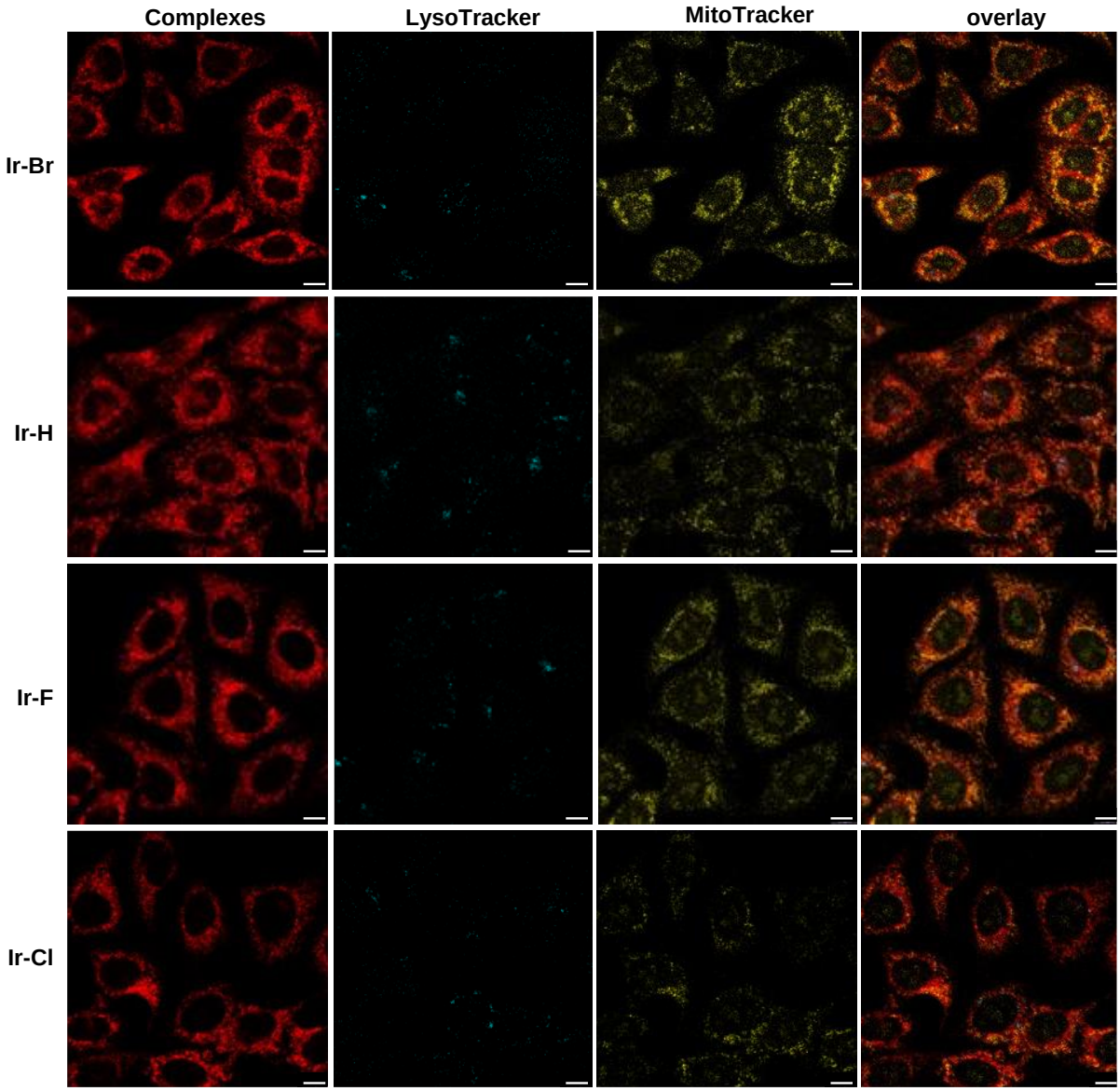

Figure S 22 : **Ir(III) complexes are colocalized with mitochondria.** Colocalization of 1 µmol.L^{-1} **Ir-Br, Ir-F, Ir-H,** or **Ir-Cl** and organelle-specific probes in HeLa cells. Compounds fluorescence (red), MitoTracker orange (yellow), LysoTracker blue (cyan). Scale bars, 10 µm.

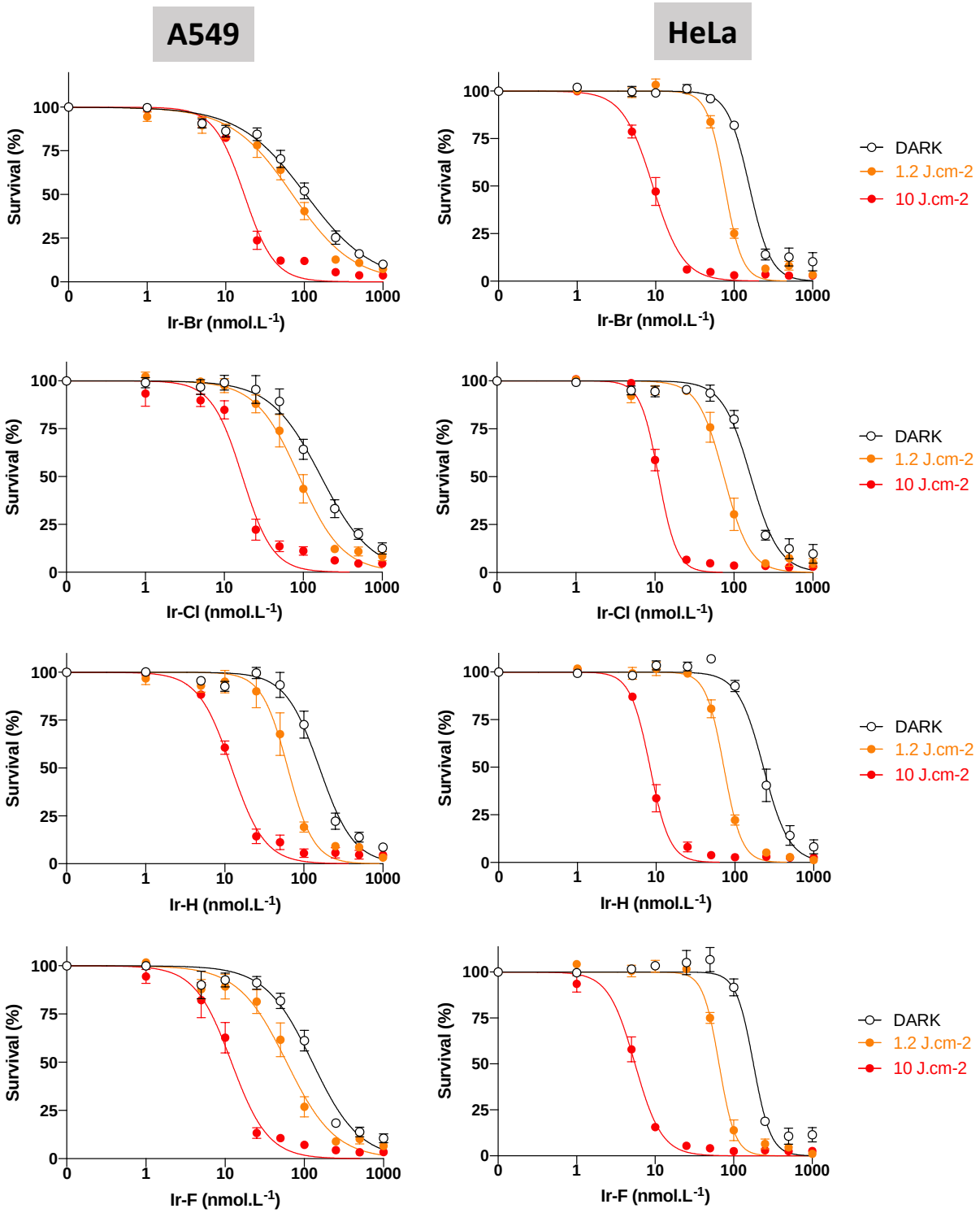

Figure S 23 : Ir(III) complexes induced phototoxicity in A549 and HeLa cells. A549 cells (left panels) and HeLa cells (right panels) were treated with increasing concentrations of **Ir-Br**, **Ir-Cl, Ir-H**, or **Ir-F** for 4 h before light exposure at 420 nm (fluency 1.2 J.cm^{-2} in orange, and 10 J.cm^{-2} in red). In parallel, cells were maintained in the dark (in black). Cell viability was assessed 72 h following light exposure. Data are expressed as the mean ± SD of 4 independent experiments performed in triplicate.

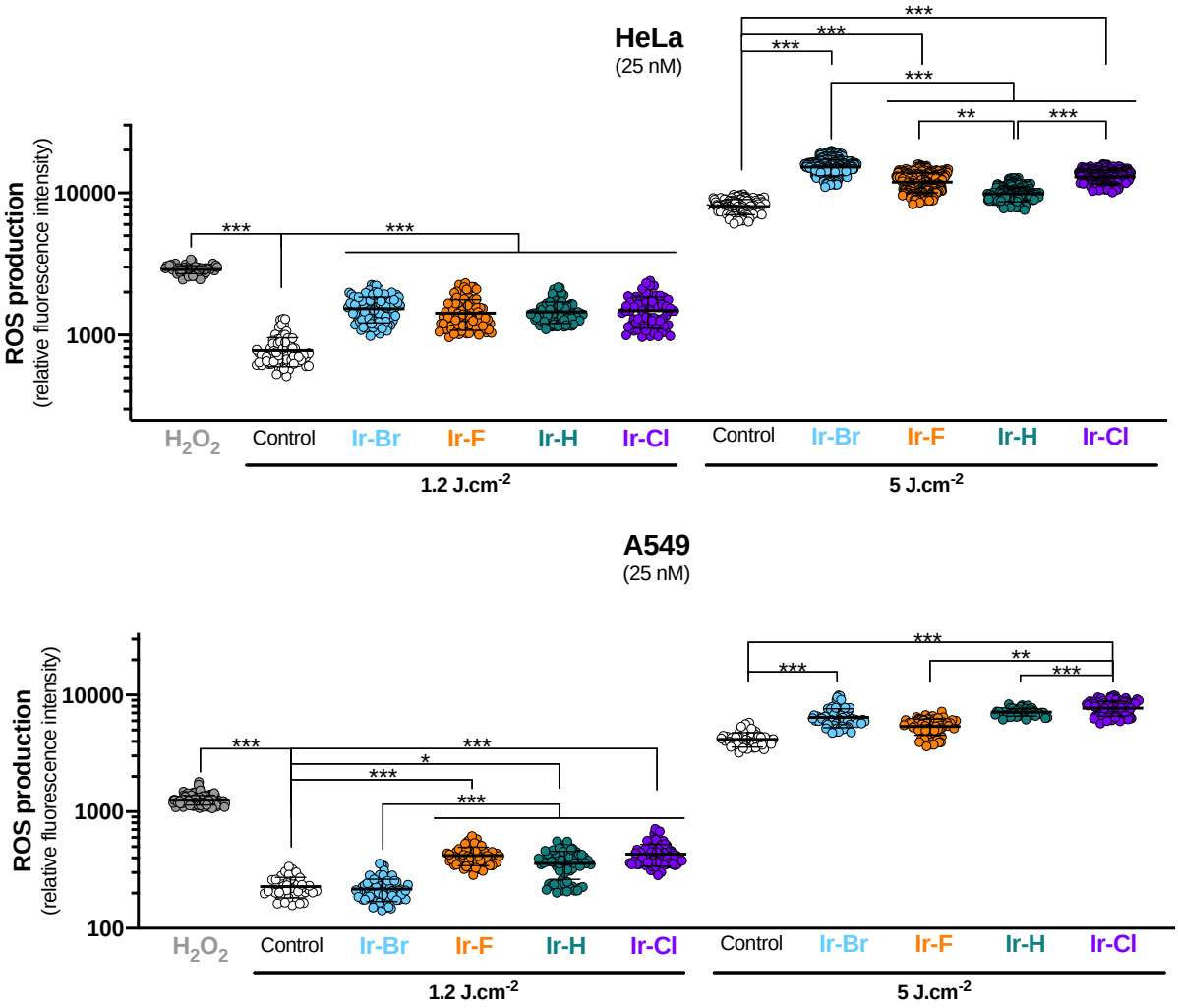

Figure S 24 : Ir(III) complexes generate cellular ROS in A549 and HeLa cells after light exposure. HeLa and A549 cells were incubated with 25 nmol.L^{-1} **Ir-Br, Ir-F, Ir-H,** or **Ir-Cl** for 4 h before light exposure at 420 nm (fluency 1.2 and 5 J.cm^{-2}) and intracellular ROS detection by DCFH-DA. Each dot represents the mean emission intensity of the DCFH-DA dye in a single cell. Bars: mean ± SD (n=2 independent experiments, performed in duplicates). 100 µmol.L^{-1} hydrogen peroxide is used as positive control.

High resolution mass spectra

The spectra were obtained on a LTQ Orbitrap XL Theme Scientific in ESI mode.

m/z	calculated for :	C17 H20 N3	$[M+H]^+$ 266.16517:
m/z	found	266.16499	
Error ppm		-0.692	

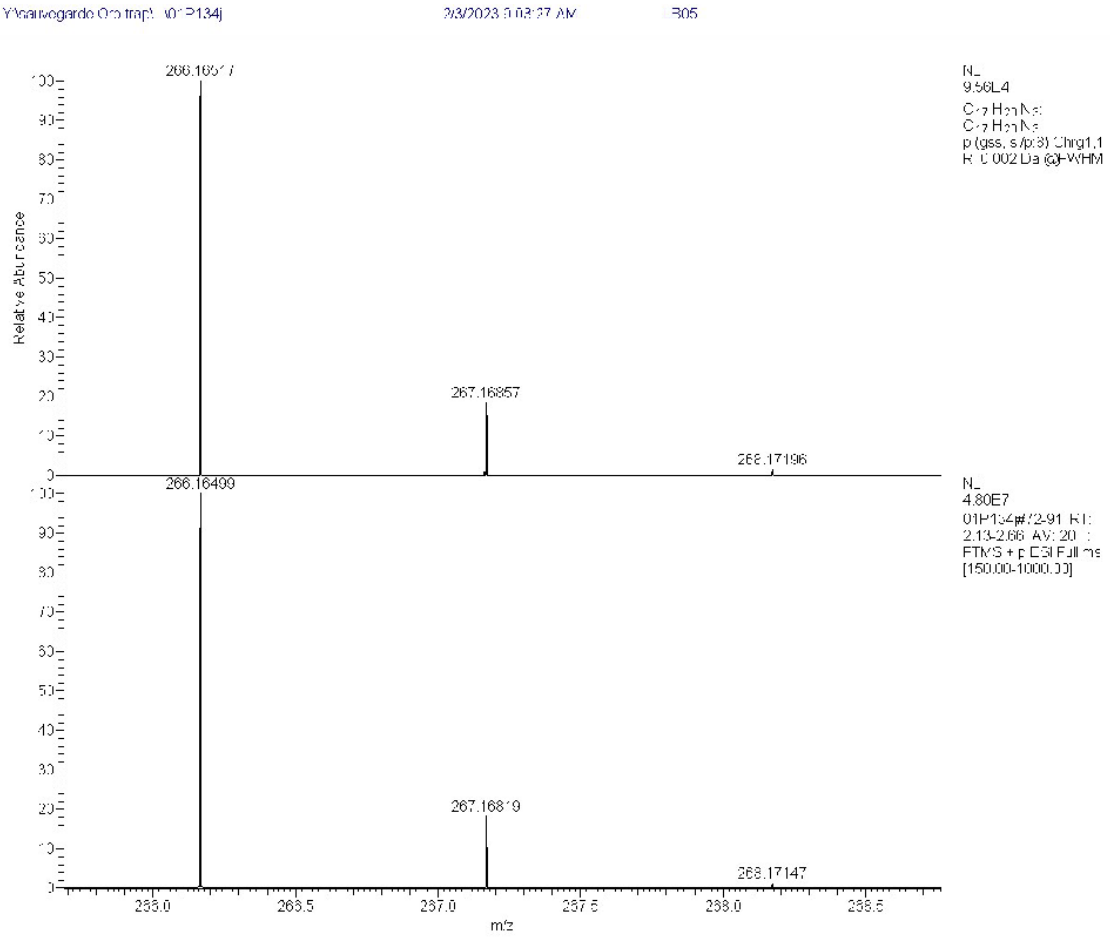

Figure S 25 : HRMS spectrum for ligand **2a**

m/z	**calculated for :**	**C17 H19 N3 F**	**$(M+H)^+$ 284.15575:**
m/z	**found**	**284.15536**	
Error ppm		**-1.381**	

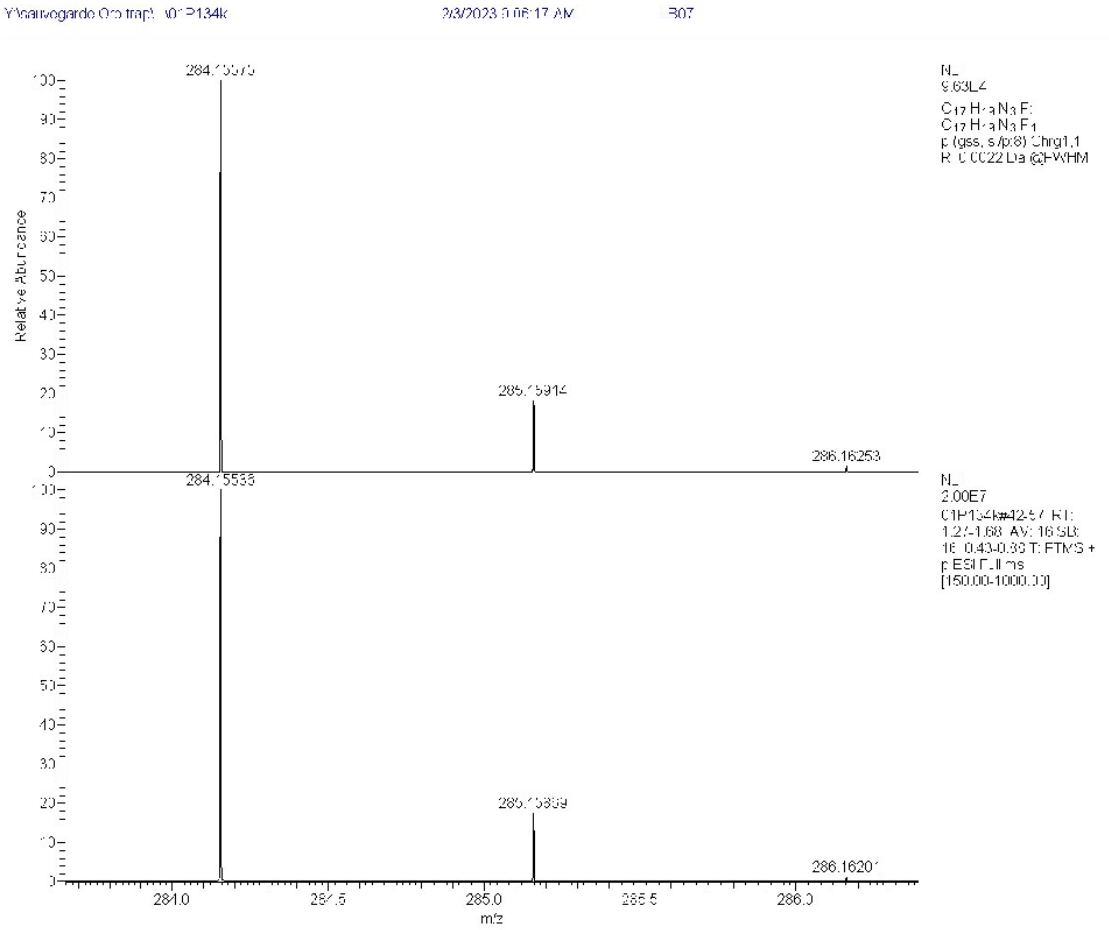

Figure S 26 : HRMS spectrum for ligand **2b**

m/z	**calculated for :**	**C17 H19 N3 Cl**	**$[M+H]^+$ 300.12620:**
m/z	**found**	**300.12568**	
Error ppm		**-1.739**	

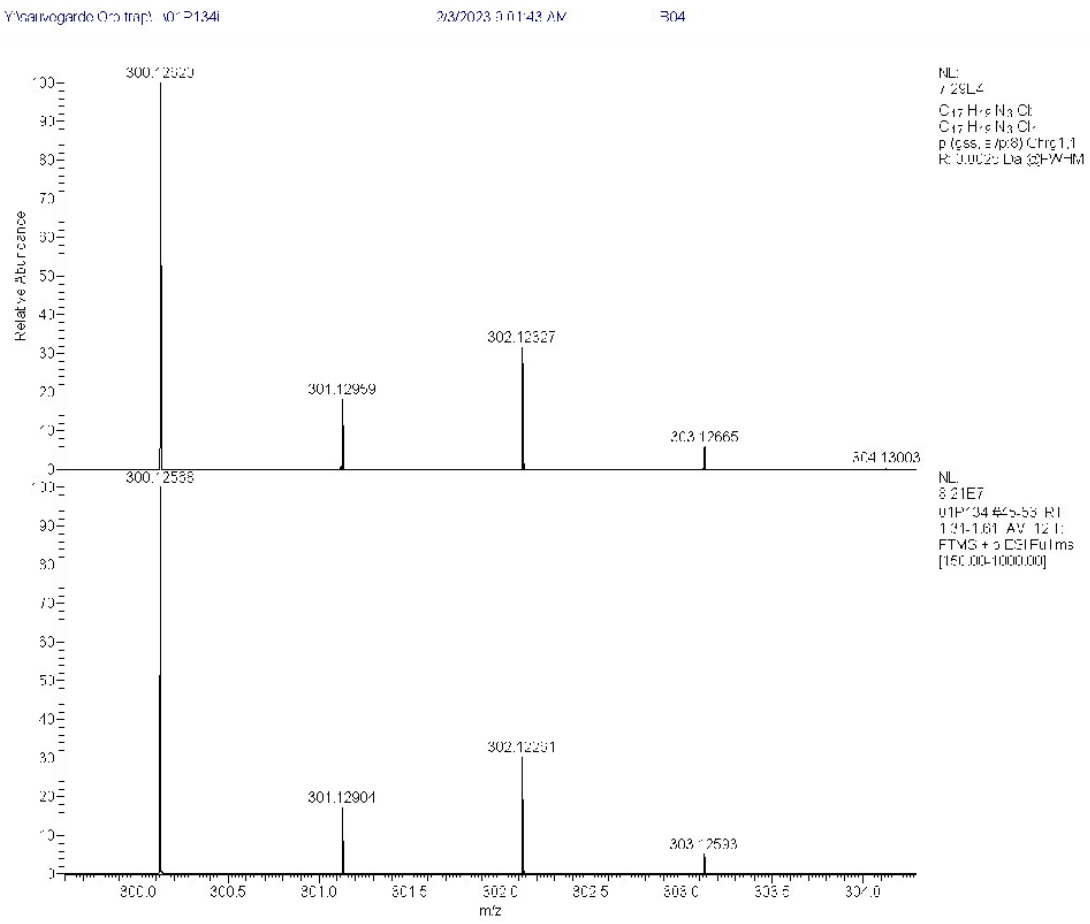

Figure S 27 : HRMS spectrum for ligand **2c**

m/z	**calculated for :**	**C39 H35 N5 Ir**	**$(M-PF_6)^+$ 766.25183:**
m/z	**found**	**766.25131**	
Error ppm		**-0.407**	

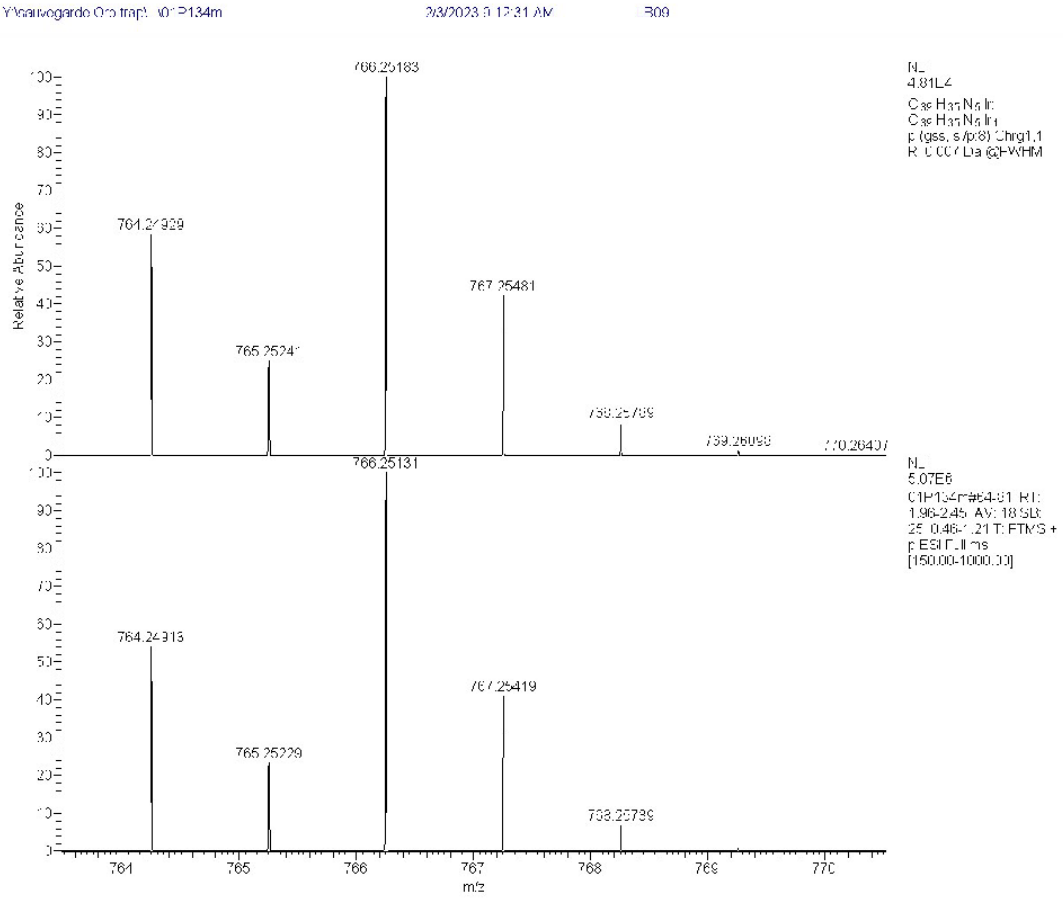

Figure S 28 : HRMS spectrum for **Ir-H**

m/z	calculated for :	C39 H34 N5 F Ir	$[M-PF6]^+$: 784.24241
m/z	found	784.24110	
Error ppm		-1.402	

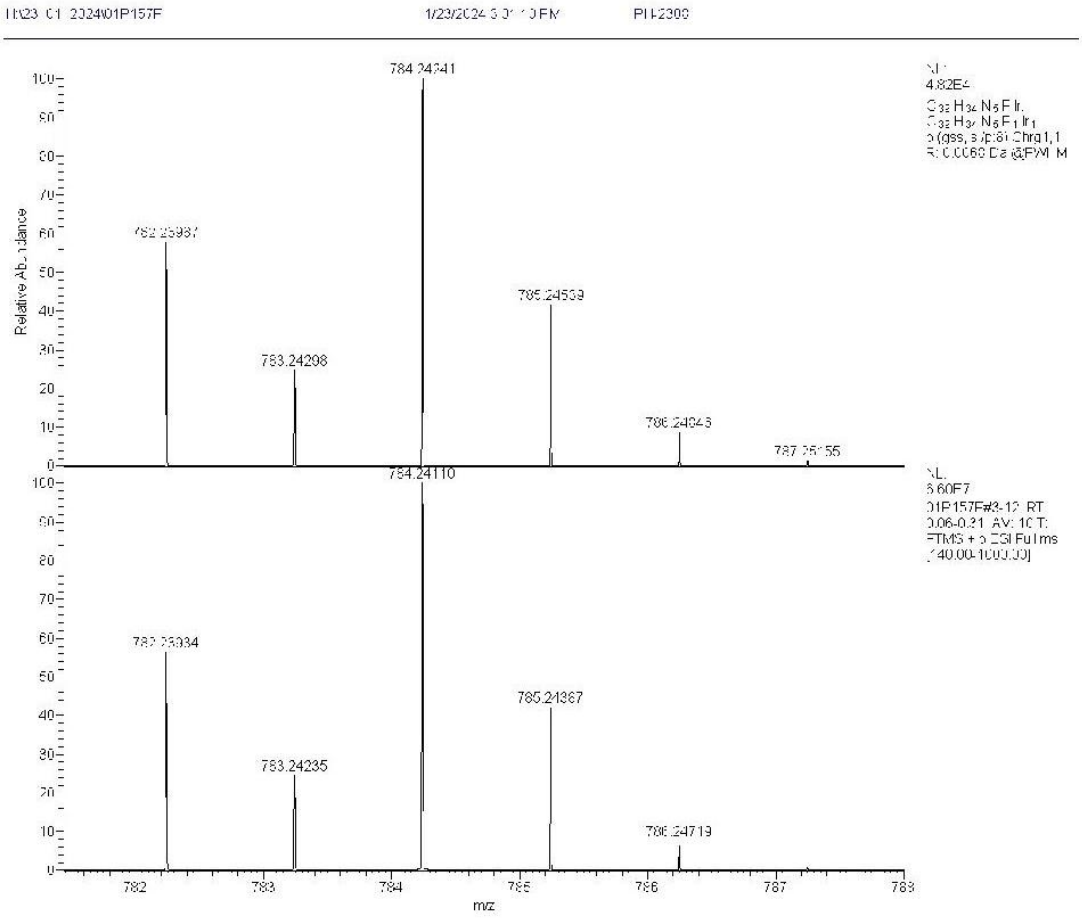

Figure S 29 : HRMS spectrum for **Ir-F**

m/z	calculated for :	C39 H34 N5 Cl Ir	$[M-PF6]^+$ 800.21202:
m/z	found	800.21146	
Error ppm		-1.486	

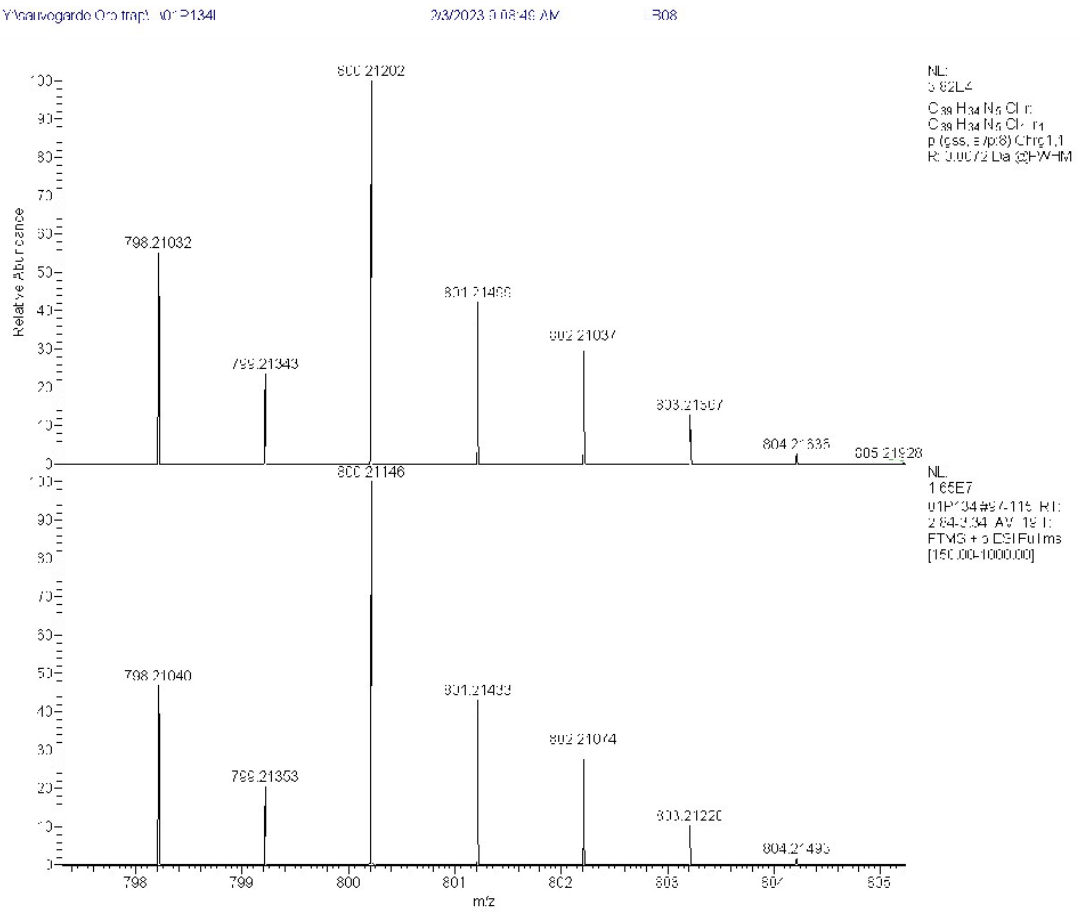

Figure S 30 : HRMS spectrum for **Ir-Cl**